Computers and Mathematics with Applications 140 (2023) 1–16

Contents lists available at ScienceDirect

Computers and Mathematics with Applications

journal homepage: www.elsevier.com/locate/camwa

Numerical solution of singularly perturbed 2-D convection-diffusion elliptic interface PDEs with Robin-type boundary conditions

Carmelo Clavero [a,*], Ram Shiromani [b], Vembu Shanthi [b]

[a] Department of Applied Mathematics, IUMA, University of Zaragoza, Zaragoza, Spain
[b] Department of Mathematics, National Institute of Technology, Tiruchirappalli, Tamilnadu, India

A R T I C L E I N F O

Keywords:
Discontinuous source term
Finite difference scheme
Shishkin mesh
Singular perturbation parameter
Elliptic equation
Two dimensional space

A B S T R A C T

We consider a singularly perturbed two-dimensional convection-diffusion elliptic interface problem with Robin boundary conditions, where the source term is a discontinuous function. The coefficient of the highest-order terms in the differential equation and in the boundary conditions, denoted by ε, is a positive parameter which can be arbitrarily small. Due to the discontinuity in the source term and the presence of the diffusion parameter, the solutions to such problems have, in general, boundary, corner and weak-interior layers. In this work, a numerical approach is carried out using a finite-difference technique defined on an appropriated layer-adapted piecewise uniform Shishkin mesh to provide a good estimate of the error. We show some numerical results which corroborate in practice that these results are sharp.

1. Introduction

Several partial differential equations (PDEs) found in practice are parameter-dependent with a singularly perturbed nature for small values of this parameter. Moreover, the solutions to these problems have boundary layers, that are almost near the boundary or at the interior of the domain where the solution possesses an extremely higher gradient. These layers can be either regular (exponential) or of parabolic type (characteristic).

Application of these problems, for simplified problems defined on rectangular domains, ranges from magnetohydrodynamic flow, simulation of oil and gas reservoirs, chemical flow reactor theory (see e.g. [1]), boundary layers influenced by suction (or blowing) of some fluid (see e.g. [2,3]). The same model is used in [4] to simulate the transport and dispersion of pollutants in a fluid or porous media. Hence, the application of numerical techniques is required to precisely solve these complicated equations. Although, classical techniques is a highly sought interesting topic of research for numerical analysts, it can completely fail in the presence of layers (see e.g. [5,6]). In a nutshell, our objective is to establish a numerical technique that can generate estimations which resolve the existing layers and for which an error bound independent of the perturbation parameter can be proven, i.e., the numerical method is uniformly convergent.

Singularly perturbed elliptic problems with Dirichlet type boundary conditions, analogous to (1.1), have been widely explored in the literature (see [7–13]). However, there are just a few research using Robin boundary conditions (RBCs) to solve the singularly perturbed 1-D problems [14–18]. To resolve the layers and build parameter-uniform numerical algorithms, all of these researches used Shishkin meshes. As far as we are aware, there is no work in the literature that considers the approximation of a singularly perturbed elliptic interface problem with Robin boundary conditions like (1.1) on layer-adaptive piecewise meshes. As a result, the goal of this study is to provide a parameter-uniform numerical technique for the problem (1.1) using a piecewise uniform mesh of Shishkin type. To preserve accuracy, the space derivative is discretized using the upwind difference scheme, and Robin boundary conditions are approximated using a finite difference scheme. We provide the suggested method's convergence analysis and prove that it is an almost first order parameter-uniform method. To validate our theoretical results and the method's efficiency, some numerical experiments are carried out.

* Corresponding author.
E-mail addresses: clavero@unizar.es (C. Clavero), ram.panday.786@gmail.com (R. Shiromani), vshanthi@nitt.edu (V. Shanthi).

https://doi.org/10.1016/j.camwa.2023.03.010
Received 13 September 2022; Received in revised form 24 February 2023; Accepted 14 March 2023

To be precise, let us define a singularly perturbed 2-D convection-diffusion elliptic interface problem with Robin boundary conditions, given by

$$\begin{cases} \mathcal{L}_\varepsilon z(x,y) = f(x,y), \quad \forall (x,y)\in\mathfrak{D}, \\ \mathcal{B}_1 z(x,y) \equiv z(x,y) - \varepsilon \dfrac{\partial z(x,y)}{\partial x} = g_1(y),\ (x,y)\in\Gamma_1, \\ \mathcal{B}_2 z(x,y) \equiv z(x,y) - \varepsilon \dfrac{\partial z(x,y)}{\partial y} = g_2(x),\ (x,y)\in\Gamma_2, \\ \mathcal{B}_3 z(x,y) \equiv z(x,y) + \varepsilon \dfrac{\partial z(x,y)}{\partial x} = g_3(y),\ (x,y)\in\Gamma_3, \\ \mathcal{B}_4 z(x,y) \equiv z(x,y) + \varepsilon \dfrac{\partial z(x,y)}{\partial y} = g_4(x),\ (x,y)\in\Gamma_4, \end{cases} \tag{1.1a}$$

where the differential operator is

$$\mathcal{L}_\varepsilon z(x,y) \equiv -\varepsilon\left(\frac{\partial^2 z}{\partial x^2}+\frac{\partial^2 z}{\partial y^2}\right) + a(x,y)\frac{\partial z}{\partial x} + b(x,y)\frac{\partial z}{\partial y} + c(x,y)z, \tag{1.1b}$$

the boundaries are

$$\Gamma_1 = \{(0,y)\,|\,(0\le y\le d_2)\cup(d_2\le y\le 1)\},\quad \Gamma_2 = \{(x,0)\,|\,(0\le x\le d_1)\cup(d_1\le x\le 1)\},$$
$$\Gamma_3 = \{(1,y)\,|\,(0\le y\le d_2)\cup(d_2\le y\le 1)\},\quad \Gamma_4 = \{(x,1)\,|\,(0\le x\le d_1)\cup(d_1\le x\le 1)\},$$

and $\Gamma = \Gamma_1\cup\Gamma_2\cup\Gamma_3\cup\Gamma_4$.

The arbitrarily small perturbation parameter satisfies $0<\varepsilon\ll 1$. The problem's domain is $\mathfrak{D} = \bigcup_{k=1}^{4}\mathfrak{D}_k$, being $\mathfrak{D}_1 = \Omega_x^-\times\Omega_y^-$, $\mathfrak{D}_2 = \Omega_x^+\times\Omega_y^-$, $\mathfrak{D}_3 = \Omega_x^-\times\Omega_y^+$, and $\mathfrak{D}_4 = \Omega_x^+\times\Omega_y^+$, where $\Omega_x^- = (0,d_1)$, $\Omega_x^+ = (d_1,1)$, $\Omega_y^- = (0,d_2)$, and $\Omega_y^+ = (d_2,1)$, and d_1, d_2 are any point in $(0,1)$. Let $\mathfrak{D}^* = (0,1)\times(0,1)$. We assume that the convection terms are bounded and they satisfy

$$a(x,y)\ge\alpha>0,\ b(x,y)\ge\beta>0,$$

for some constants α and β, while the reaction coefficient satisfies $c(x,y)\ge 0$. We also suppose that $a|_{\mathfrak{D}}, b|_{\mathfrak{D}}\in C^{3,\gamma}(\mathfrak{D})$, $f|_{\mathfrak{D}_k}\in C^{3,\gamma}(\mathfrak{D}_k)$, $c\in C^{3,\gamma}(\bar{\mathfrak{D}})$, and $g_k\in C^{4,\gamma}(\mathfrak{D})$, for some $\gamma\in(0,1]$, $k=1,2,3,4$. Further, we assume that the data of the problem satisfy sufficient compatibility conditions (see, the reference [9]). Hence, $z\in C^{4,\gamma}(\mathfrak{D}_k)$, $k=1,2,3,4$ (see [19,20]). We denote the continuous subsets of the boundaries and the interior line segments of the discontinuity by $\Gamma_{k,j}$, $c_{k,j}$, where $j=1,2,3,4$ indicate the edges and corners of $\mathfrak{D}_k$, respectively.

In problem (1.1), the source term $f(x,y)$ has a jump discontinuity at both lines $x=d_1$ and $y=d_2$. So, it is congruent to denote the jump discontinuity in any function κ at a point $(x,y)\in\mathfrak{D}$ along the lines parallel to x- and y-axes as $[\kappa](d_1,y) = \kappa(d_1^+,y)-\kappa(d_1^-,y)$ and $[\kappa](x,d_2) = \kappa(x,d_2^+)-\kappa(x,d_2^-)$ respectively.

The paper is organized as follows. In Section 2, we express the maximum principle, the boundedness of the continuous solution, and prove adequate estimates for its derivatives. In Section 3, we construct the numerical approach by using a finite difference scheme (FDS) defined on an adequate Shishkin mesh. In section 4, we derive the error estimation proving that the numerical scheme is an almost first-order uniformly convergent method; in a future, we have the intention to analyze the uniform convergence of the numerical method defined on other special meshes, such as Bakhvalov, Gartland or Duran-Shishkin meshes. Also, we are sure that it is interesting to consider the case when a posteriori meshes are used, which are based on appropriated error indicators; note that, from a numerical point of view, these meshes are useful because they can be constructed without information on the behaviour of the exact solution of the continuous problem. Finally, in Section 5 some test problems are solved and the numerical results corroborate in practice the theoretical results.

Henceforth, we denote by $\|\cdot\|_D$ the maximum norm on the domain D; moreover, C denotes a generic positive constant which is independent of the diffusion parameter ε and the discretization parameter N.

2. Analytical properties of the solution

The present section contains the maximum principle for the differential operator, along with consequent stability results, and bounds on the solution and its derivatives.

Theorem 2.1. *(Maximum principle) Let the function $\Phi\in C^1(\mathfrak{D}^*)\cap C^2(\mathfrak{D})$ such that $\mathcal{B}_i\Phi(x,y)\ge 0$ on Γ_i, $i=1,2,3,4$, $\mathcal{L}_\varepsilon\Phi(x,y)\ge 0$ for all $(x,y)\in\mathfrak{D}$, $\left[\dfrac{\partial\Phi}{\partial x}\right](d_1,y)\le 0$, and $\left[\dfrac{\partial\Phi}{\partial y}\right](x,d_2)\le 0$. Then $\Phi(x,y)\ge 0$ for all $(x,y)\in\bar{\mathfrak{D}}$.*

Proof. We follow the technique used in [21]. Consider the function $\mathcal{V}$ on $\bar{\mathfrak{D}}$ defined through $\Phi(x,y) = \mathcal{V}(x,y)\psi(x,y)$, with the function

$$\psi(x,y) = \exp\left(\frac{\alpha(x-d_1)}{2\varepsilon}+\frac{\beta(y-d_2)}{2\varepsilon}\right),\quad (x,y)\in\bar{\mathfrak{D}},$$

where $\alpha>0$, and $\beta>0$ are some constants. Let be $\mathcal{V}(x',y') = \min_{(x,y)\in\bar{\mathfrak{D}}}\{\mathcal{V}(x,y)\}$. If $\mathcal{V}(x',y')\ge 0$, there is nothing to prove. Suppose $\mathcal{V}(x',y')<0$. We distinguish several cases.

Case(i): If $(x',y')\in\mathfrak{D}$, at the point (x',y'), it holds $\dfrac{\partial\mathcal{V}}{\partial x}(x',y') = \dfrac{\partial\mathcal{V}}{\partial y}(x',y') = 0$ and $\dfrac{\partial^2\mathcal{V}}{\partial x^2}(x',y')\ge 0$, $\dfrac{\partial^2\mathcal{V}}{\partial y^2}(x',y')\ge 0$. Then, we have

$$\mathcal{L}_\varepsilon\Phi(x',y') = \psi(x',y')\Bigg(-\varepsilon\Delta\mathcal{V} + \left(\frac{\alpha}{2\varepsilon}\Big(-\frac{\alpha}{2}+a(x',y')\Big)+\frac{\beta}{2\varepsilon}\Big(-\frac{\beta}{2}+b(x',y')\Big)\right)\mathcal{V}(x',y')$$

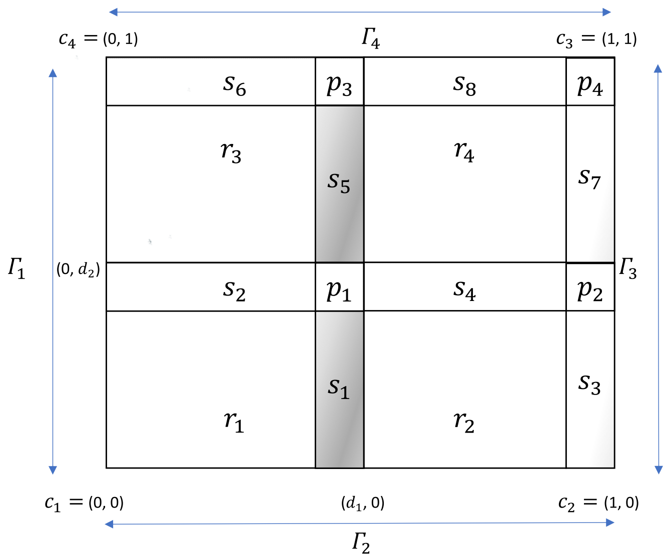

Fig. 1. Layer appearance diagram.

$$+c(x',y')\mathcal{V}(x',y')\Big) < 0,$$

which contradicts the hypothesis.

Case(ii): If $(x',y') \in \Gamma_1$, the left boundary along the y-direction, we have that $\dfrac{\partial \mathcal{V}}{\partial x} \geq 0$ implies that $\dfrac{\partial \Phi}{\partial x} \geq 0$. Hence,

$$\mathcal{B}_1\Phi(x',y') \equiv \Phi(x',y') - \varepsilon \frac{\partial \Phi(x',y')}{\partial x} < 0,$$

which contradicts the hypothesis.

Case(iii): If $(x',y') \in \Gamma_3$, the right boundary along the y-direction, we have that $\dfrac{\partial \mathcal{V}}{\partial x} \leq 0$ implies that $\dfrac{\partial \Phi}{\partial x} \leq 0$. Hence

$$\mathcal{B}_3\Phi(x',y') \equiv \Phi(x',y') + \varepsilon \frac{\partial \Phi(x',y')}{\partial x} < 0,$$

which contradicts the hypothesis.

Similarly, at the other two boundaries, that is, if $(x',y') \in \Gamma_2 \cup \Gamma_4$, it can be proved that we also arrive at contradiction.

Case(iv): If $(x',y') \in \{(d_1,y) \cup (x,d_2)\}$. Here, either $(x',y') = (d_1,y')$, or $(x',y') = (x',d_2)$. Let us consider $(x',y') = (d_1,y')$. Given $\mathcal{V}$ takes minimum value at (x',y'), then $\dfrac{\partial \mathcal{V}}{\partial x}(d_1^+,y') \geq 0$ and $\dfrac{\partial \mathcal{V}}{\partial x}(d_1^-,y') \leq 0$. Then, it is evident that $\left[\dfrac{\partial \mathcal{V}}{\partial x}\right] \geq 0$. As $\mathcal{V}(d_1,y') < 0$, we have

$$\left[\frac{\partial \Phi}{\partial x}\right](d_1,y') = \exp\left(\frac{\beta(y'-d_2)}{2\varepsilon}\right)\left(\left[\frac{\partial \mathcal{V}}{\partial x}\right](d_1,y')\right) > 0,$$

contradicting the hypothesis $\dfrac{\partial \Phi}{\partial x}(d_1,y) \leq 0$.

The another case when $(x',y') = \{(x',d_2)\}$ can be proved similarly. This completes the proof. $\square$

A consequence of this maximum principle is the parameter uniform boundedness of the solution of (1.1) given below.

Lemma 2.2 *(Stability result). Let $z(x,y)$ be the solution of (1.1). Then, Theorem 2.1 holds, and yields the stability estimate*

$$\|z(x,y)\| \leq \frac{1}{K}\|f\|_{\bar{\mathfrak{D}}} + \max_{(x,y)\in\bar{\mathfrak{D}}}\Big\{|g_1(y)|, |g_2(x)|, |g_3(y)|, |g_4(x)|\Big\}, \tag{2.1}$$

where $K = \min(\alpha,\beta)$.

Proof. We define the smooth barrier function

$$\psi^{\pm}(x,y) = \begin{cases} M + \frac{\|f\|_{\bar{\mathfrak{D}}}}{K}\left(1 + \frac{x}{d_1} + \frac{y}{d_2}\right) \pm z(x,y), & (x,y) \in [0,d_1]\times[0,d_2], \\ M + \frac{\|f\|_{\bar{\mathfrak{D}}}}{K}\left(1 + \frac{(1-x)}{(1-d_1)} + \frac{y}{d_2}\right) \pm z(x,y), & (x,y) \in (d_1,1]\times[0,d_2], \\ M + \frac{\|f\|_{\bar{\mathfrak{D}}}}{K}\left(1 + \frac{x}{d_1} + \frac{(1-y)}{(1-d_2)}\right) \pm z(x,y), & (x,y) \in [0,d_1]\times(d_2,1], \\ M + \frac{\|f\|_{\bar{\mathfrak{D}}}}{K}\left(1 + \frac{(1-x)}{(1-d_1)} + \frac{(1-y)}{(1-d_2)}\right) \pm z(x,y), & (x,y) \in (d_1,1]\times(d_2,1], \end{cases} \tag{2.2}$$

where $M = \max_{(x,y)\in\bar{\mathfrak{D}}} \left\{ |g_1(y)|, |g_2(x)|, |g_3(y)|, |g_4(x)| \right\}$.
Thus, clearly $\mathcal{B}_i\psi(x,y) \geq 0$ on Γ_i, $i = 1,2,3,4$. For all $(x,y) \in \mathfrak{D}$, we have $\mathcal{L}_\varepsilon\psi^\pm(x,y) \geq 0$. Since, $z(x,y) \in C^1(\mathfrak{D}^*) \cup C^2(\mathfrak{D})$, we have

$$\left[\frac{\partial\psi^\pm}{\partial x}\right](d_1,y) = \frac{-\|f\|_{\bar{\mathfrak{D}}}}{d_1(1-d_1)K} \pm \left[\frac{\partial z^\pm}{\partial x}\right](d_1,y) \leq 0,$$
$$\left[\frac{\partial\psi^\pm}{\partial y}\right](x,d_2) = \frac{-\|f\|_{\bar{\mathfrak{D}}}}{d_2(1-d_2)K} \pm \left[\frac{\partial z^\pm}{\partial y}\right](x,d_2) \leq 0.$$

From the discrete maximum principle, it follows that $\psi^\pm(x,y) \geq 0$, $\forall (x,y) \in \bar{\mathfrak{D}}$, which allows to get the required bound on $\|z(x,y)\|_{\bar{\mathfrak{D}}}$. □

We state the following global bounds on the solution's derivatives. They follow from arguments in [22,23].

Lemma 2.3. *Let z be the solution of (1.1). Then, for $0 \leq i+j \leq 4$,*

$$\left\|\frac{\partial^{i+j} z}{\partial x^i \partial y^j}\right\|_{\mathfrak{D}_k} \leq C\varepsilon^{-(i+j)},\ k = 1,2,3,4. \tag{2.3}$$

Proof. We consider the new variables $\varsigma = (1-x)/\varepsilon$, $\eta = (1-y)/\varepsilon$; in the new variables, the continuous problem is given by

$$\begin{cases} \dfrac{\partial^2 z}{\partial\varsigma^2} + \dfrac{\partial^2 z}{\partial\eta^2} - a(\varsigma,\eta)\dfrac{\partial z}{\partial\varsigma} - b(\varsigma,y)\dfrac{\partial z}{\partial\eta} + \varepsilon c(\varsigma,\eta)z, = \varepsilon f(\varsigma,\eta), \quad \forall(\varsigma,\eta) \in \mathfrak{D}_\varepsilon, \\ z(\varsigma,\eta) + \dfrac{\partial z(\varsigma,\eta)}{\partial\varsigma} = g_1(\eta),\ (\varsigma,\eta) \in \Gamma_{1,\varepsilon}, \\ z(\varsigma,\eta) + \dfrac{\partial z(\varsigma,\eta)}{\partial\eta} = g_2(\varsigma),\ (\varsigma,\eta) \in \Gamma_{2,\varepsilon}, \\ z(\varsigma,\eta) - \dfrac{\partial z(,\varsigma,\eta)}{\partial\varsigma} = g_3(\eta),\ (\varsigma,\eta) \in \Gamma_{3,\varepsilon}, \\ z(\varsigma,\eta) - \dfrac{\partial z(\varsigma,\eta)}{\partial\eta} = g_4(\varsigma),\ (\varsigma,\eta) \in \Gamma_{4,\varepsilon}, \end{cases}$$

where $\mathfrak{D}_\varepsilon = (0, \frac{1}{\varepsilon})^2$ and $\Gamma_{i,\varepsilon}$, $i = 1,2,3,4$ are the corresponding boundaries of $\mathfrak{D}_\varepsilon$. Then, from [24] it follows that

$$\left\|\frac{\partial^{i+j} z}{\partial\varsigma^i \partial\eta^j}\right\|_{\mathfrak{D}_k} \leq C,\ k = 1,2,3,4,$$

and therefore, in the original variables, (2.3) follows. □

To get pointwise bounds, we start by proposing a solution decomposition of the solution of (1.1). Here, to establish stronger bounds on the smooth components r_k, $k = 1,2,3,4$, we will do the analysis separately for the subregions $\mathfrak{D}_k$, $k = 1,2,3,4$. To accomplish this, we first investigate the subregion $\mathfrak{D}_1$ and introduce a new function r_1^* on the domain $\bar{\Omega}^*$ which is a sufficiently large neighbourhood of $\bar{\mathfrak{D}}_1$ such that $\bar{\mathfrak{D}}_1 \subset \bar{\mathfrak{D}}_1^*$. Define an extended domain, for example $\mathfrak{D}_1^* = (0, d_1+\rho_1) \times (0, d_2+\rho_2)$, where $\rho_1, \rho_2 > 0$ with $\Gamma^* = \bar{\mathfrak{D}}_1^* \backslash \mathfrak{D}_1^*$, corners c_k^* and edges Γ_k^*, $k = 1,2,3,4$. Suppose that the regular component r_1^* defined on $\bar{\mathfrak{D}}_1^*$ can be decomposed as $r_1^* = r_{0,1}^* + \varepsilon r_{1,1}^* + \varepsilon^2 r_{2,1}^*$, where $r_{k,1}^*$, $k = 0,1$ are the solution of the following first-order problems

$$\begin{cases} a^*\dfrac{\partial r_{0,1}^*}{\partial x} + b^*\dfrac{\partial r_{0,1}^*}{\partial y} + c^* r_{0,1}^* = f^*, \quad \forall(x,y) \in \mathfrak{D}_1^*, \\ \mathcal{B}_1 r_{0,1}^*(x,y) = \mathcal{B}_1 z(x,y),\ \forall(x,y) \in \Gamma_1^*,\ \mathcal{B}_2 r_{0,1}^*(x,y) = \mathcal{B}_2 z(x,y),\ \forall(x,y) \in \Gamma_2^*, \\ a^*\dfrac{\partial r_{1,1}^*}{\partial x} + b^*\dfrac{\partial r_{1,1}^*}{\partial y} + c^* r_{1,1}^* = \left(\dfrac{\partial^2}{\partial x^2} + \dfrac{\partial^2}{\partial y^2}\right) r_{0,1}, \quad \forall(x,y) \in \mathfrak{D}_1^*, \\ \mathcal{B}_k r_{1,1}^*(x,y) = 0,\ \forall(x,y) \in \Gamma_k^*,\ k = 1,2, \end{cases} \tag{2.4}$$

and $r_{2,1}^*$ is the solution of the boundary value problem

$$\begin{cases} -\varepsilon\left(\dfrac{\partial^2 r_{2,1}^*}{\partial x^2} + \dfrac{\partial^2 r_{2,1}^*}{\partial y^2}\right) + a^*\dfrac{\partial r_{2,1}^*}{\partial x} + b^*\dfrac{\partial r_{2,1}^*}{\partial y} + c^* r_{2,1}^* = \left(\dfrac{\partial^2}{\partial x^2} + \dfrac{\partial^2}{\partial y^2}\right) r_{1,1}^*, \quad \forall(x,y) \in \mathfrak{D}_1^*, \\ \mathcal{B}_k r_{2,1}^*(x,y) = 0,\ (x,y) \in \Gamma_k^*,\ k = 1,2,3,4. \end{cases} \tag{2.5}$$

Here, the coefficients a^*, b^*, c^* and f^* are respective smooth extensions of the functions a, b, c and f associated with the problem (1.1) from the domain $\bar{\mathfrak{D}}_1$ onto the domain $\bar{\mathfrak{D}}_1^*$. Since, $r_{1,1}^* \in C^{4,\gamma}(\mathfrak{D}_1^*)$, we get

$$\left(\frac{\partial^2}{\partial x^2} + \frac{\partial^2}{\partial y^2}\right) r_{1,1}^* \in C^{2,\gamma}(\mathfrak{D}_1^*).$$

The extension of all the functions are taken such that the compatibility conditions at the corners of the $\bar{\mathfrak{D}}_1^*$ up to second order (see [9,19]) are satisfied. Hence $r_{2,1}^* \in C^{4,\gamma}(\mathfrak{D}_1^*)$.
The regular component r_1, is taken to be the solution of the boundary value problem

$$\mathcal{L}_\varepsilon r_1(x,y) = f(x,y),\ \forall(x,y) \in \mathfrak{D}_1, \tag{2.6a}$$

$$\mathcal{B}_k r_1(x,y) = \mathcal{B}_k r_1^*(x,y), \quad \forall(x,y) \in \Gamma_{1,j},\ j,k = 1,2, \tag{2.6b}$$

$$r_1(x,y)=0, \quad \forall (x,y)\in \Gamma_{1,j},\ j=3,4. \tag{2.6c}$$

Applying Lemma 2.2 and Lemma 2.3 to the extended problem (2.5), we deduce that $r_1 \in C^{4,\gamma}(\mathfrak{D}_1)$ and

$$\left\|\frac{\partial^{k+l} r_1}{\partial x^k \partial y^l}\right\|_{\mathfrak{D}_1} \le C(1+\varepsilon^{2-(k+l)}), \quad 0\le k+l\le 4. \tag{2.7}$$

Similarly, corresponding to the remaining subdomains $\mathfrak{D}_k$, $k=2,3,4$, we can define the remaining smooth functions r_k, $k=2,3,4$.

Corresponding to the right edge Γ_3 of the domain $\mathfrak{D}_4$, a regular layer component s_7 exists, which is the solution of the problem

$$\mathcal{L}_\varepsilon s_7 = 0, \quad \forall (x,y)\in \mathfrak{D}_4, \tag{2.8a}$$

$$s_7(x,y)=0,\ \forall (x,y)\in \Gamma_{4,1}\cup\Gamma_{4,2}, \tag{2.8b}$$

$$\mathcal{B}_3 s_7(x,y)=g_3(y),\ \forall (x,y)\in \Gamma_{4,3},\ \mathcal{B}_4 s_7(x,y)=0,\ \forall (x,y)\in\Gamma_{4,4}. \tag{2.8c}$$

To obtain the bound for s_7, we consider the transformed function $\overline{s}_7$. Set $\varsigma=(1-x)/\varepsilon$ and $s_7(x,y)=\overline{s}_7(\varsigma,y)$. We write $\overline{\mathcal{L}}_\varepsilon$ for the operator $\mathcal{L}_\varepsilon$ defined in term of the variables ς and y. Then,

$$\overline{\mathcal{L}}_\varepsilon \overline{s}_7(\varsigma,y) = -\varepsilon^{-1}\frac{\partial^2 \overline{s}_7}{\partial \varsigma^2} - \varepsilon\frac{\partial^2 \overline{s}_7}{\partial y^2} - \varepsilon^{-1}\overline{a}(\varsigma,y)\frac{\partial \overline{s}_7}{\partial \varsigma} + \overline{b}(\varsigma,y)\frac{\partial \overline{s}_7}{\partial y} + \overline{c}(\varsigma,y)\overline{s}_7,$$

where, $\overline{a}(\varsigma,y)=a(1-\varepsilon\varsigma,y)$, $\overline{b}(\varsigma,y)=b(1-\varepsilon\varsigma,y)$ and $\overline{c}(\varsigma,y)=c(1-\varepsilon\varsigma,y)$. Expanding $\overline{a}(\varsigma,y)$, $\overline{b}(\varsigma,y)$ and $\overline{c}(\varsigma,y)$ in powers of $\varepsilon\varsigma$, using Taylor series, we have

$$\overline{a}(\varsigma,y)=\sum_{l=0}^{\infty}\frac{(-\varepsilon\varsigma)^l}{l!}\frac{\partial^l a}{\partial x^l}(1,y),\ \overline{b}(\varsigma,y)=\sum_{l=0}^{\infty}\frac{(-\varepsilon\varsigma)^l}{l!}\frac{\partial^l b}{\partial x^l}(1,y),$$
$$\overline{c}(\varsigma,y)=\sum_{l=0}^{\infty}\frac{(-\varepsilon\varsigma)^l}{l!}\frac{\partial^l c}{\partial x^l}(1,y).$$

.

The solution $\bar{s}_7$ of the equation $\bar{\mathcal{L}}_\varepsilon \bar{s}_7=0$ is expanded into powers of ε, as $\overline{s}_7=\overline{s}_{0,7}+\varepsilon\overline{s}_{1,7}$. With the above change of variables, equating the coefficients of ε^0 and ε^{-1} in $\overline{s}_7$ for $(\varsigma,y)\in(0,(1-d_1)/\varepsilon)\times(0,1)$, that solves (2.8), we deduce that $\overline{s}_{0,7}$ and $\overline{s}_{1,7}$, satisfy the second order differential equations

$$\frac{\partial^2 \overline{s}_{0,7}}{\partial\varsigma^2}+a(1,y)\frac{\partial \overline{s}_{0,7}}{\partial\varsigma}=0, \tag{2.9a}$$

$$\frac{\partial^2 \overline{s}_{1,7}}{\partial\varsigma^2}+a(1,y)\frac{\partial \overline{s}_{1,7}}{\partial\varsigma}=b(1,y)\frac{\partial \overline{s}_{0,7}}{\partial y}+c(1,y)\overline{s}_{0,7}+\varsigma\frac{\partial a(1,y)}{\partial x}\frac{\partial \overline{s}_{0,7}}{\partial\varsigma}=0, \tag{2.9b}$$

with boundary conditions

$$\mathcal{B}_1\overline{s}_{e,7}(0,y)=-\mathcal{B}_3 r_{e,7}(1,y),\ \mathcal{B}_3\overline{s}_{e,7}(\varsigma,y)\to 0 \quad as \quad \varsigma\to\infty,\ e=0,1. \tag{2.9c}$$

Solving (2.9), we obtain

$$\overline{s}_{0,7}(\varsigma,y)=(-\mathcal{B}_3 r_{0,7}(1,y))\exp(-a(1,y)\varsigma),$$

and

$$\overline{s}_{1,7}(\varsigma,y)=\big\{-\mathcal{B}_3 r_{1,7}+\varsigma\big[\frac{\partial}{\partial y}\big(\frac{b}{a}\mathcal{B}_3 r_{0,7}\big)+\frac{c-a}{a}\mathcal{D}_3 r_{0,7}\big]+\varsigma^2\big[\frac{b}{a}\frac{\partial a}{\partial y}+\frac{\partial a}{\partial x}\big](\mathcal{B}_3 r_{0,7})\big\}(1,y)\exp(-a(1,y)\varsigma).$$

Using that $\min\limits_{(x,y)\in\overline{\mathfrak{D}}} a(x,y)>\alpha$, it follows

$$\left|\frac{\partial^{k+l}\overline{s}_{e,7}}{\partial x^k\partial y^l}\right|\le C\varepsilon^{-k-l}\exp(-\alpha\varsigma), \quad 0\le k+l\le 4, \quad e=0,1,$$

and hence

$$\left|\frac{\partial^{k+l} s_{e,7}}{\partial x^k\partial y^l}\right|\le C\varepsilon^{-k-l}\exp(-\alpha(1-x)/\varepsilon), \quad 0\le k+l\le 4, \quad e=0,1.$$

This implies that the bounds on the regular boundary layer component are

$$\left|\frac{\partial^{k+l} s_7}{\partial x^k\partial y^l}\right|\le C\varepsilon^{-k-l}\exp(-\alpha(1-x)/\varepsilon), \quad 0\le k+l\le 4. \tag{2.10}$$

In view of $s_7\in C^{3,\gamma}((0,(1-d_1)/\varepsilon)\times(0,1))$, an analogue of (2.3) applies to s_7 in $(0,(1-d_1)/\varepsilon)\times(0,1)$, implies another desired bound

$$\left\|\frac{\partial^l s_7}{\partial y^l}\right\|\le C\varepsilon^{1-l}, \quad 0\le l\le 4. \tag{2.11}$$

Similarly, corresponding to the remaining domain's edge $\Gamma_{k,j}$ of the domains $\mathfrak{D}_k$, $k=1,2,3,4$ we can define remaining boundary and interior layer components s_i, $i=1,2,...6,8$ (see Fig. 1).

Next we introduce the corner layer component p_4 (see, Fig. 1) related to the corner $(1,1)$ of the domain $\mathfrak{D}_4$, which is the solution of the boundary value problem

$$\mathcal{L}_\varepsilon p_4(x,y)=0, \quad \forall (x,y)\in\mathfrak{D}_4, \tag{2.12a}$$

$$\mathcal{B}_3 p_4(x,y)=-\mathcal{B}_3 s_7(x,y),\ \forall (x,y)\in\Gamma_{4,3}, \quad \mathcal{B}_4 p_4(x,y)=-\mathcal{B}_4 s_8(x,y),\ \forall (x,y)\in\Gamma_{4,4}, \tag{2.12b}$$

$$p_4(x,y)=0,\ \forall (x,y)\in\Gamma_{4,1}\cup\Gamma_{4,2}. \tag{2.12c}$$

We note that $\mathcal{L}_\varepsilon s_7=\mathcal{L}_\varepsilon s_8=0$ and $s_7, s_8\in C^{4,\gamma}(\mathfrak{D}_4)$. Therefore, the compatibility conditions up to second-order exist at the four corners of the domain which indicates that $p_4\in C^{4,\gamma}(\mathfrak{D}_4)$ (see [9,19]). Now, set $\varsigma=(1-x)/\varepsilon$, $\eta=(1-y)/\varepsilon$ and the corner layer component $p_4(x,y)=\breve{p}_4(\varsigma,\eta)$ in (2.12) corresponding to p_4. Furthermore, we write $\breve{\mathcal{L}}_\varepsilon$ for the operator $\mathcal{L}_\varepsilon$ defined in terms of the variables ς and η. Then, we have

$$\breve{\mathcal{L}}_\varepsilon \breve{p}_4(\varsigma,\eta)=-\varepsilon^{-1}\Big(\frac{\partial^2\breve{p}_4}{\partial\varsigma^2}+\frac{\partial^2\breve{p}_4}{\partial\eta^2}\Big)+\breve{a}(\varsigma,\eta)\varepsilon^{-1}\frac{\partial\breve{p}_4}{\partial\varsigma}+\breve{b}(\varsigma,\eta)\varepsilon^{-1}\frac{\partial\breve{p}_4}{\partial\eta}+\breve{c}(\varsigma,\eta)\breve{p}_4,$$

where, $\breve{a}(\varsigma,\eta)=a(1-\varepsilon\varsigma,1-\varepsilon\eta)$, $\breve{b}(\varsigma,\eta)=b(1-\varepsilon\varsigma,1-\varepsilon\eta)$ and $\breve{c}(\varsigma,\eta)=c(1-\varepsilon\varsigma,1-\varepsilon\eta)$. Expanding $\breve{a}(\varsigma,\eta)$, $\breve{b}(\varsigma,\eta)$ and $\breve{c}(\varsigma,\eta)$ in powers of $\varepsilon\varsigma$ and $\varepsilon\eta$ using Taylor series, we have

$$\breve{a}(\varsigma,\eta)=\sum_{l=0}^{\infty}\sum_{m=0}^{\infty}\frac{(-\varepsilon\varsigma)^l(-\varepsilon\eta)^m}{l!m!}\frac{\partial^{l+m}a}{\partial x^l\partial y^m}(1,1),$$

$$\breve{b}(\varsigma,\eta)=\sum_{l=0}^{\infty}\sum_{m=0}^{\infty}\frac{(-\varepsilon\varsigma)^l(-\varepsilon\eta)^m}{l!m!}\frac{\partial^{l+m}b}{\partial x^l\partial y^m}(1,1),$$

$$\breve{c}(\varsigma,\eta)=\sum_{l=0}^{\infty}\sum_{m=0}^{\infty}\frac{(-\varepsilon\varsigma)^l(-\varepsilon\eta)^m}{l!m!}\frac{\partial^{l+m}c}{\partial x^l\partial y^m}(1,1).$$

Let $\breve{p}_4=\breve{p}_{0,4}+\varepsilon\breve{p}_{1,4}$, where $\breve{p}_{e,4}$, for $e=0,1$ are the solutions of the second order differential equations

$$\frac{\partial^2\breve{p}_{0,4}}{\partial\varsigma^2}+\frac{\partial^2\breve{p}_{0,4}}{\partial\eta^2}+a(1,1)\frac{\partial\breve{p}_{0,4}}{\partial\varsigma}+b(1,1)\frac{\partial\breve{p}_{0,4}}{\partial\eta}=0,$$

and

$$\frac{\partial^2\breve{p}_{1,4}}{\partial\varsigma^2}+\frac{\partial^2\breve{p}_{1,4}}{\partial\eta^2}-\varsigma\frac{\partial a(1,1)}{\partial x}\frac{\partial\breve{p}_{0,4}}{\partial\varsigma}-\eta\frac{\partial a(1,1)}{\partial y}\frac{\partial\breve{p}_{0,4}}{\partial\varsigma}-\varsigma\frac{\partial b(1,1)}{\partial x}\frac{\partial\breve{p}_{0,4}}{\partial\eta}-\eta\frac{\partial b(1,1)}{\partial y}\frac{\partial\breve{p}_{0,4}}{\partial\eta}$$
$$+a(1,1)\frac{\partial\breve{p}_{1,4}}{\partial\varsigma}+b(1,1)\frac{\partial\breve{p}_{1,4}}{\partial\eta}-c(1,1)\breve{p}_{0,1}=0,$$

on $(\varsigma,\eta)\in(0,(1-d_1)/\varepsilon)\times(0,(1-d_2)/\varepsilon)$, respectively, which satisfy the boundary conditions

$$\mathcal{B}_2\breve{p}_{e,4}(\varsigma,0)=-\mathcal{B}_4 r_{e,4}(\varsigma,1),\ \mathcal{B}_1\breve{p}_{e,4}(0,\eta)=-\mathcal{B}_3 r_{e,4}(1,\eta),\ \mathcal{B}_k\breve{p}_{e,4}(\varsigma,\eta)\to 0,\ k=3,4,$$

as $\varsigma,\eta\to\infty$, for $e=0,1$. Following the arguments in [9], we can deduce

$$\left|\frac{\partial^{k+l}p_4}{\partial x^k\partial y^l}\right|\le C\varepsilon^{-k-l}\exp(-\alpha(1-x)/\varepsilon)\exp(-\beta(1-y)/\varepsilon),\ 0\le k+l\le 4.$$

In view of $p_4\in C^{3,\gamma}((0,(1-d_1)/\varepsilon)\times(0,(1-d_2)/\varepsilon))$, an analogue of (2.3) applies to p_4 in $(0,(1-d_1)/\varepsilon)\times(0,(1-d_2)/\varepsilon)$, implies another desired bound

$$\left\|\frac{\partial^{k+l}p_4}{\partial x^k\partial y^l}\right\|\le C\varepsilon^{-k-l}, \quad 0\le k+l\le 4.$$

Next, we introduce the corner layer component p_1 (see, Fig. 1) of the domain $\mathfrak{D}_1$, which is the solution of the boundary value problem

$$\mathcal{L}_\varepsilon p_1(x,y)=0, \quad \forall (x,y)\in\mathfrak{D}_1, \tag{2.13a}$$

$$\mathcal{B}_1 p_1(x,y)=0,\ \forall (x,y)\in\Gamma_{1,1}, \quad \mathcal{B}_2 p_1(x,y)=0,\ \forall (x,y)\in\Gamma_{1,2}, \tag{2.13b}$$

$$p_1(x,y)=-s_1(x,y),\ \forall (x,y)\in\Gamma_{1,3}, \quad p_1(x,y)=-s_2(x,y),\ \forall (x,y)\in\Gamma_{1,4}. \tag{2.13c}$$

To obtain the bound for p_1, we use Lemma 2.1 and the barrier function $\Psi\pm p_1$, where

$$\Psi(x,y)=C\frac{\epsilon^2}{\alpha\beta}\exp\Big(-\frac{\alpha(d_1-x)}{\epsilon}\Big)\exp\Big(-\frac{\beta(d_2-y)}{\epsilon}\Big).$$

Let p_1 satisfies (2.13) and we can prove the derivative bounds for p_1 over the domain $\mathfrak{D}_1$ with the help of [25,26], using similar arguments to those ones given in the previous proof for p_4.

Similarly we can be describe the bounds of the remaining corner layer components p_k, $k=2,3$ related to the remaining corners of the domains $\mathfrak{D}_k$, $k=2,3$.

As a result, we have created a Shishkin solution decomposition and calculated the derivatives of its components. Local Schauder-type estimates ([25], p.110, (1.12) and (1.13)) can be used in place of the global bound ([25], p.110, (1.11)) to derive more precise pointwise bounds on the derivatives of the layer components, which contain decaying exponential factors.

From previous estimates, we can now conclude with the following theorem, which gives the decomposition of the exact solution and show its asymptotic behaviour with respect to the diffusion parameter ε.

Theorem 2.4. *The exact solution z of the continuous problem (1.1) may be written as a sum*

$$z=\sum_{i=1}^{4} r_i+\sum_{j=1}^{8} s_j+\sum_{k=1}^{4} p_k,$$

where,

$$\mathcal{L}_\varepsilon r_i=f,\quad \mathcal{L}_\varepsilon s_j=0,\quad \mathcal{L}_\varepsilon p_k=0,\quad i,k=1,\dots 4,\ j=1,\dots,8.$$

The boundary conditions for regular, regular boundary layer and corner layer components can be expressed so that the following bounds on the derivatives of the components hold

$$\left\|\frac{\partial^{k+l} r_i}{\partial x^k\partial y^l}\right\|\le C(1+\varepsilon^{2-(k+l)}),\quad 0\le k+l\le 4.$$

$$\begin{aligned}
&|s_1(x,y)|\le C\varepsilon e^{\frac{-\alpha}{\varepsilon}|d_1-x|}, && |s_2(x,y)|\le C\varepsilon e^{\frac{-\beta}{\varepsilon}|d_2-y|},\\
&|s_3(x,y)|\le C e^{\frac{-\alpha}{\varepsilon}(1-x)}, && |s_4(x,y)|\le C\varepsilon e^{\frac{-\beta}{\varepsilon}|d_2-y|},\\
&|s_5(x,y)|\le C\varepsilon e^{\frac{-\alpha}{\varepsilon}|d_1-x|}, && |p_1(x,y)|\le C\varepsilon^2 e^{\frac{-\alpha}{\varepsilon}|d_1-x|}e^{\frac{-\beta}{\varepsilon}|d_2-y|},\\
&|s_6(x,y)|\le C e^{\frac{-\beta}{\varepsilon}(1-y)}, && |p_2(x,y)|\le C\varepsilon e^{\frac{-\alpha}{\varepsilon}(1-x)}e^{\frac{-\beta}{\varepsilon}|d_2-y|},\\
&|s_7(x,y)|\le C e^{\frac{-\alpha}{\varepsilon}(1-x)}, && |p_3(x,y)|\le C\varepsilon e^{\frac{-\alpha}{\varepsilon}|d_1-x|}e^{\frac{-\beta}{\varepsilon}(1-y)},\\
&|s_8(x,y)|\le C e^{\frac{-\beta}{\varepsilon}(1-y)}; && |p_4(x,y)|\le C e^{\frac{-\alpha}{\varepsilon}(1-x)}e^{\frac{-\beta}{\varepsilon}(1-y)},
\end{aligned}$$

$$\begin{cases}
\left\|\frac{\partial^k s_i}{\partial x^k}\right\|\le C\varepsilon^{1-k},\ \left\|\frac{\partial^l s_i}{\partial y^l}\right\|\le C\varepsilon^{2-l},\ \textit{where},\ 0\le k,l\le 4,\ i=1,5,\\
\left\|\frac{\partial^l s_i}{\partial y^l}\right\|\le C\varepsilon^{1-l},\ \left\|\frac{\partial^k s_i}{\partial x^k}\right\|\le C\varepsilon^{2-k},\ \textit{where},\ 0\le k,l\le 4,\ i=2,4,\\
\left\|\frac{\partial^k s_i}{\partial x^k}\right\|\le C\varepsilon^{-k},\ \left\|\frac{\partial^l s_i}{\partial y^l}\right\|\le C\varepsilon^{1-l},\ \textit{where},\ 0\le k,l\le 4,\ i=3,7,\\
\left\|\frac{\partial^l s_i}{\partial y^l}\right\|\le C\varepsilon^{-l},\ \left\|\frac{\partial^k s_i}{\partial x^k}\right\|\le C\varepsilon^{1-k},\ \textit{where},\ 0\le k,l\le 4,\ i=6,8,\\
\left\|\frac{\partial^{k+l} p_1}{\partial x^k\partial y^l}\right\|\le C\varepsilon^{2-k-l},\ \left\|\frac{\partial^{k+l} p_4}{\partial x^k\partial y^l}\right\|\le C\varepsilon^{-k-l},\quad \textit{where}\ 0\le k+l\le 4,\\
\left\|\frac{\partial^{k+l} p_j}{\partial x^k\partial y^l}\right\|\le C\varepsilon^{1-k-l},\quad \textit{where}\ 0\le k+l\le 4,\ j=2,3.
\end{cases}$$

3. Discretization of the problem

3.1. The Shishkin mesh

Motivate by the solution decomposition in Theorem 2.4, we construct a suitable piecewise uniform fitted mesh as follows. First, we define the mesh transition points,

$$\tau_x=\min\left\{\frac{d_1}{2},\frac{2\varepsilon}{\alpha}\ln N\right\},\ \text{and}\ \tau_y=\min\left\{\frac{d_2}{2},\frac{2\varepsilon}{\beta}\ln N\right\}. \tag{3.1}$$

Then, we subdivide the unit intervals in x into four subdomains

$$[0,1]=[0,d_1-\tau_x]\cup[d_1-\tau_x,d_1]\cup[d_1,1-\tau_x]\cup[1-\tau_x,1]. \tag{3.2a}$$

Note that the grid points around the interior points d_1 and d_2, are concentrated only in the left part and not in the right part, which is the same that it occurs in [21].

Let $\bar{\mathfrak{D}}_x^N$ then denote the one-dimensional piecewise uniform mesh obtained by placing a uniform mesh with $N/4$ mesh intervals on each of the four subdomains in (3.2a). For convenience, we denote $\mathfrak{D}_x^N$ the mesh points in $\bar{\mathfrak{D}}_x^N$ that exclude the boundary and discontinuity points $\{0,d_1,1\}$. Similarly, we subdivide the unit intervals in y into four subintervals

$$[0,1]=[0,d_2-\tau_y]\cup[d_2-\tau_y,d_2]\cup[d_2,1-\tau_y]\cup[1-\tau_y,1]. \tag{3.2b}$$

Let $\bar{\mathfrak{D}}_y^N$ then denote the one-dimensional piecewise uniform mesh obtained by placing a uniform mesh on each of the subintervals in (3.2b), with N/4 mesh intervals. Again, for convenience, we denote $\mathfrak{D}_y^N\equiv\bar{\mathfrak{D}}_y^N\backslash\{0,d_2,1\}$. Finally, we set $\bar{\mathfrak{D}}^{N,N}=\bar{\mathfrak{D}}_x^N\times\bar{\mathfrak{D}}_y^N$. Therefore, $\bar{\mathfrak{D}}^{N,N}$ is the piecewise two-dimensional tensor product mesh with grid points (x_i,y_j) where $x_i\in\bar{\mathfrak{D}}_x^N$, $y_j\in\bar{\mathfrak{D}}_y^N$. Similarly, we set $\mathfrak{D}^{N,N}=\mathfrak{D}_x^N\times\mathfrak{D}_y^N$.

The interior regions of the mesh are denoted by $\mathfrak{D}^{N,N} = \bigcup_{k=1}^{4} \mathfrak{D}_k^{N,N}$. Here the subdomains are

$$\mathfrak{D}_1^{N,N} = \left\{ (x_i, y_j) : 1 \le i \le \left(\frac{N}{2} - 1\right), 1 \le j \le \left(\frac{N}{2} - 1\right) \right\};$$
$$\mathfrak{D}_2^{N,N} = \left\{ (x_i, y_j) : \left(\frac{N}{2} + 1\right) \le i \le (N-1), 1 \le j \le \left(\frac{N}{2} - 1\right) \right\};$$
$$\mathfrak{D}_3^{N,N} = \left\{ (x_i, y_j) : 1 \le i \le \left(\frac{N}{2} - 1\right), \left(\frac{N}{2} + 1\right) \le j \le (N-1) \right\};$$
$$\mathfrak{D}_4^{N,N} = \left\{ (x_i, y_j) : \left(\frac{N}{2} + 1\right) \le i \le (N-1), \left(\frac{N}{2} + 1\right) \le j \le (N-1) \right\}.$$

The boundaries of these subdomains are denoted as

$$\Gamma_1^{N,N} = \left\{ (0, y_j) \Big| \left(0 \le j < \frac{N}{2}\right) \cup \left(\frac{N}{2} < j \le N\right) \right\},$$
$$\Gamma_2^{N,N} = \left\{ (x_i, 0) \Big| \left(0 \le i < \frac{N}{2}\right) \cup \left(\frac{N}{2} < i \le N\right) \right\},$$
$$\Gamma_3^{N,N} = \left\{ (1, y_j) \Big| \left(0 \le j < \frac{N}{2}\right) \cup \left(\frac{N}{2} < j \le N\right) \right\},$$
$$\Gamma_4^{N,N} = \left\{ (x_i, 1) \Big| \left(0 \le i < \frac{N}{2}\right) \cup \left(\frac{N}{2} < i \le N\right) \right\},$$

and $\Gamma^{N,N} = \Gamma_1^{N,N} \cup \Gamma_2^{N,N} \cup \Gamma_3^{N,N} \cup \Gamma_4^{N,N}$.
We shall employ the notation that $h_i = x_i - x_{i-1}$, and $k_j = y_j - y_{j-1}$. But since there are few actual distinct mesh widths, it is useful to introduce notation for them:

$$h_i = \begin{cases} H_l = \dfrac{4(d_1 - \tau_x)}{N}, & i = 1, \dots, \dfrac{N}{4}, \\ h_l = \dfrac{4\tau_x}{N}, & i = \dfrac{N}{4} + 1, \dots, \dfrac{N}{2}, \\ H_r = \dfrac{4(1 - \tau_x - d_1)}{N}, & i = \dfrac{N}{2} + 1, \dots, \dfrac{3N}{4}, \\ h_r = \dfrac{4\tau_x}{N}, & i = \dfrac{3N}{4} + 1, \dots, N, \end{cases}$$
$$k_j = \begin{cases} K_l = \dfrac{4(d_2 - \tau_y)}{N}, & i = 1, \dots, \dfrac{N}{4}, \\ k_l = \dfrac{4\tau_y}{N}, & i = \dfrac{N}{4} + 1, \dots, \dfrac{N}{2}, \\ K_r = \dfrac{4(1 - \tau_y - d_2)}{N}, & i = \dfrac{N}{2} + 1, \dots, \dfrac{3N}{4}, \\ k_r = \dfrac{4\tau_y}{N}, & i = \dfrac{3N}{4} + 1, \dots, N. \end{cases} \tag{3.3}$$

3.2. The finite difference scheme (FDS)

On the previous piecewise-uniform mesh $\bar{\mathfrak{D}}^{N,N}$, we consider the finite-difference operator

$$\begin{cases} \mathcal{L}_\varepsilon^{N,N} Z(x_i, y_j) & \equiv -\varepsilon(\delta_{xx}^2 + \delta_{yy}^2) Z(x_i, y_j) + a_{i,j} D_x^- Z(x_i, y_j) + b_{i,j} D_y^- Z(x_i, y_j) + c_{i,j} Z(x_i, y_j) \\ & = f_{i,j}, \ \forall (x_i, y_j) \in \mathfrak{D}^{N,N}, \\ \mathcal{B}_1^{N,N} Z(x_i, y_j) & \equiv Z(x_i, y_j) - \varepsilon D_x^+ Z(x_i, y_j) = g_1(y_j), \text{ for } (x_i, y_j) \in \Gamma_1^{N,N}, \\ \mathcal{B}_2^{N,N} Z(x_i, y_j) & \equiv Z(x_i, y_j) - \varepsilon D_y^+ Z(x_i, y_j) = g_2(x_i), \text{ for } (x_i, y_j) \in \Gamma_2^{N,N}, \\ \mathcal{B}_3^{N,N} Z(x_i, y_j) & \equiv Z(x_i, y_j) + \varepsilon D_x^- Z(x_i, y_j) = g_3(y_j), \text{ for } (x_i, y_j) \in \Gamma_3^{N,N}, \\ \mathcal{B}_4^{N,N} Z(x_i, y_j) & \equiv Z(x_i, y_j) + \varepsilon D_y^- Z(x_i, y_j) = g_4(x_i), \text{ for } (x_i, y_j) \in \Gamma_4^{N,N}, \end{cases} \tag{3.4a}$$

and the discretization at the points (d_1, y_j) and (x_i, d_2) is given by

$$\begin{cases} D_x^- Z(x_{N/2}, y_j) = D_x^+ Z(x_{N/2}, y_j), \\ D_y^- Z(x_i, y_{N/2}) = D_y^+ Z(x_i, y_{N/2}), \end{cases} \tag{3.4b}$$

respectively, where the discrete differential operators D_x^-, D_x^+, D_y^-, D_y^+, δ_{xx}^2, and δ_{yy}^2 are defined in classical way as follows:

$$\begin{cases} D_x^- Z(x_i, y_j) = \frac{Z(x_i, y_j) - Z(x_{i-1}, y_j)}{h_i}, \quad D_x^+ Z(x_i, y_j) = \frac{Z(x_{i+1}, y_j) - Z(x_i, y_j)}{h_{i+1}}, \\ D_y^- Z(x_i, y_j) = \frac{Z(x_i, y_j) - Z(x_i, y_{j-1})}{k_j}, \quad D_y^+ Z(x_i, y_j) = \frac{Z(x_i, y_{j+1}) - Z(x_i, y_j)}{k_{j+1}}, \\ \delta_{xx}^2 Z(x_i, y_j) = \frac{1}{h_i}(D_x^+ - D_x^-) Z(x_i, y_j), \quad \delta_{yy}^2 Z(x_i, y_j) = \frac{1}{k_j}(D_y^+ - D_y^-) Z(x_i, y_j). \end{cases}$$

Lemma 3.1. *(Discrete maximum principle) The operator $\mathcal{L}_\varepsilon \Phi^{N,N}$ defined by (3.4) satisfies a discrete maximum principle, i.e. if $\mathcal{V}(x_i, y_j)$ is a mesh function that satisfies $\mathcal{B}_k^{N,N}\mathcal{V}(x_i, y_j) \geq 0$, for all $(x_i, y_j) \in \Gamma^{N,N}$, $\mathcal{L}_\varepsilon^{N,N}\mathcal{V}(x_i, y_j) \geq 0$, for all $(x_i, y_j) \in \mathfrak{D}^{N,N}$, and $D_x^+\mathcal{V}(x_{N/2}, y_j) - D_x^-\mathcal{V}(x_{N/2}, y_j) \leq 0$, $D_y^+\mathcal{V}(x_i, y_{N/2}) - D_y^-\mathcal{V}(x_i, y_{N/2}) \leq 0$ Then, $\mathcal{V}(x_i, y_j) \geq 0$, for all $(x_i, y_j) \in \bar{\mathfrak{D}}^{N,N}$.*

Proof. Let be $\mathcal{V}(x_{k_1}, y_{k_2}) = \min_{(x_i,y_j)\in\bar{\mathfrak{D}}^{N,N}} \{\mathcal{V}(x_{k_1}, y_{k_2})\}$. If $\mathcal{V}(x_{k_1}, y_{k_2}) \geq 0$, there is nothing to prove. Suppose $\mathcal{V}(x_{k_1}, y_{k_2}) < 0$. At the point $(x_i, y_j) = (x_{k_1}, y_{k_2})$, it holds

$$D_x^-\mathcal{V}(x_{k_1}, y_{k_2}) \leq 0 \leq D_x^+\mathcal{V}(x_{k_1}, y_{k_2}),\ D_y^-\mathcal{V}(x_{k_1}, y_{k_2}) \leq 0 \leq D_y^+\mathcal{V}(x_{k_1}, y_{k_2}).$$

Assume that $(x_i, y_j) \in \mathfrak{D}^{N,N}$. Then, we have

$$\mathcal{L}_\varepsilon^{N,N}\mathcal{V}(x_{k_1}, y_{k_2}) = \Big(-\varepsilon\big(\delta_{xx}^2 + \delta_{yy}^2\big)\mathcal{V} + a_{i,j}D_x^-\mathcal{V} + b_{i,j}D_y^-\mathcal{V} + c_{i,j}\mathcal{V}\Big)(x_{k_1,y_{k_2}}) < 0,$$

which contradicts the hypothesis $\mathcal{L}_\varepsilon^{N,N}\mathcal{V}(x_{k_1}, y_{k_2}) \geq 0$, for $(x_i, y_j) \in \mathfrak{D}^{N,N}$. Also at the boundary points $(x_i, y_j) = (0, y_{k_2}) \in \Gamma_1^{N,N}$, we have

$$\mathcal{B}_1^{N,N}\mathcal{V}(0, y_{k_2}) \equiv \mathcal{V}(0, y_{k_2}) - \varepsilon D_x^+\mathcal{V}(0, y_{k_2}) < 0,$$

which contradicts the hypothesis. At the other three boundary conditions when $(x_i, y_j) \in \Gamma_2^{N,N} \cup \Gamma_3^{N,N} \cup \Gamma_4^{N,N}$ it can be proved similarly. If $(x_{k_1}, y_{k_2}) \in (x_{N/2}, y_j) \cup (x_i, y_{N/2})$, we use an analogous argument. Therefore, $\mathcal{V}(x_i, y_j) \geq 0$ for all $(x_i, y_j) \in \bar{\mathfrak{D}}^{N,N}$. □

Lemma 3.2. *Let $Z_{i,j}$ be the solution of (3.4). Then, Theorem 3.1 holds and it yields the stability estimate*

$$||Z_{i,j}|| \leq \frac{1}{K}||f_{i,j}|| + \max_{(x_i,y_j)\in\partial\mathfrak{D}^{N,N}} \Big\{ |Z(x_i, y_j)| \Big\}, \tag{3.5}$$

where $K = \min\{\alpha, \beta\}$.

Proof. It can be proved easily using Lemma 3.1. □

4. Analysis of the uniform convergence

In this section we prove that the method given in (3.4), constructed on the Shishkin mesh given by the tensorial product of meshes defined in (3.3), is uniformly convergent with respect to the diffusion parameter ε. We split the discrete solution of (3.4) equivalent to the exact solution, in order to bound the nodal error independently outside and inside the layers. First, the mesh functions R_k, $k = 1, 2, 3, 4$ are the solutions of the following discrete problems:

$$\begin{cases} \mathcal{L}_\varepsilon^{N,N} R_k(x_i, y_j) = f(x_i, y_j), \quad \text{for all}\,(x_i, y_j) \in \mathcal{D}^{N,N},\ k = 1, 2, 3, 4, \\ \mathcal{B}_k^{N,N} R_k(x_i, y_j) = \mathcal{B}_k r_k(x_i, y_j), \quad \text{for all } (x_i, y_j) \in \Gamma_k^{N,N}, \\ R_k(x_{N/2}, y_j) = r_k(d_1, y_j),\ R_k(x_i, y_{N/2}) = r_k(x_i, d_2). \end{cases} \tag{4.1}$$

Hence, we defined the mesh functions S_l and P_m, $l = 1, 2, ..., 8, m = 1, 2, 3, 4$ as the solutions of the following discrete problems:

$$\begin{cases} \mathcal{L}_\varepsilon^{N,N} S_l(x_i, y_j) = 0, \quad \text{for all}\,(x_i, y_j) \in \mathcal{D}_k^{N,N},\ l = 1, ..., 8,\ k = 1, 2, 3, 4, \\ \mathcal{B}_n^{N,N} S_l(x_i, y_j) = 0, \quad \text{for all } (x_i, y_j) \in \Gamma_{1,n}^{N,N},\ n = 1, 2,\ l = 1, 2, \\ \mathcal{B}_n^{N,N} S_l(x_i, y_j) = 0, \quad \text{for all } (x_i, y_j) \in \Gamma_{2,n}^{N,N},\ n = 2, 3,\ l = 4, \\ \mathcal{B}_n^{N,N} S_l(x_i, y_j) = 0, \quad \text{for all } (x_i, y_j) \in \Gamma_{3,n}^{N,N},\ n = 1, 4,\ l = 5, \\ \mathcal{B}_2^{N,N} S_l(x_i, y_j) = 0, \quad \text{for all } (x_i, y_j) \in \Gamma_{2,2}^{N,N},\ l = 3, \\ \mathcal{B}_4^{N,N} S_l(x_i, y_j) = 0, \quad \text{for all } (x_i, y_j) \in \Gamma_{3,4}^{N,N},\ l = 6, \\ \mathcal{B}_3^{N,N} S_l(x_i, y_j) = \mathcal{B}_3 s_l(x_i, y_j), \quad \text{for all } (x_i, y_j) \in \Gamma_{k,3}^{N,N},\ k = 2, 4,\ l = 3, 7, \\ \mathcal{B}_4^{N,N} S_l(x_i, y_j) = \mathcal{B}_4 s_l(x_i, y_j), \quad \text{for all } (x_i, y_j) \in \Gamma_{k,4}^{N,N},\ k = 3, 4,\ l = 6, 8, \\ S_1(d_1, y_j) + R_1(d_1, y_j) = S_3(d_1, y_j) + R_2(d_1, y_j),\ S_5(d_1, y_j) + R_3(d_1, y_j) = S_7(d_1, y_j) + R_4(d_1, y_j), \\ S_2(x_i, d_2) + R_1(x_i, d_2) = S_6(x_i, d_2) + R_3(x_i, d_2),\ S_4(x_i, d_2) + R_2(x_i, d_2) = S_8(x_i, d_2) + R_4(x_i, d_2), \\ D_x^- S_1(d_1, y_j) + D_x^- R_1(d_1, y_j) = D_x^+ S_3(d_1, y_j) + D_x^+ R_2(d_1, y_j), \\ D_x^- S_5(d_1, y_j) + D_x^- R_3(d_1, y_j) = D_x^+ S_7(d_1, y_j) + D_x^+ R_4(d_1, y_j), \\ D_y^- S_2(x_i, d_2) + D_y^- R_1(x_i, d_2) = D_y^+ S_6(x_i, d_2) + D_y^+ R_3(x_i, d_2), \\ D_y^- S_4(x_i, d_2) + D_y^- R_2(x_i, d_2) = D_y^+ S_8(x_i, d_2) + D_y^+ R_4(x_i, d_2). \end{cases} \tag{4.2}$$

$$\begin{cases} \mathcal{L}_\varepsilon^{N,N} P_m(x_i,y_j)=0, \quad \text{for all } (x_i,y_j)\in \mathcal{D}_k^{N,N}, \ m=1,2,3,4, \ k=1,2,3,4, \\ \mathcal{B}_n^{N,N} P_1(x_i,y_j)=0, \quad \text{for all } (x_i,y_j)\in \Gamma_{1,n}^{N,N}, \ n=1,2, \\ \mathcal{B}_n^{N,N} P_2(x_i,y_j)=0, \quad \text{for all } (x_i,y_j)\in \Gamma_{2,n}^{N,N}, \ n=2, \\ \mathcal{B}_n^{N,N} P_3(x_i,y_j)=0, \quad \text{for all } (x_i,y_j)\in \Gamma_{3,n}^{N,N}, \ n=1, \\ \mathcal{B}_3^{N,N} P_2(x_i,y_j)=-\mathcal{B}_3^{N,N} S_3(x_i,y_j), \ \mathcal{B}_3^{N,N} P_4(x_i,y_j)=-\mathcal{B}_3^{N,N} S_7(x_i,y_j), \quad \text{for all } (x_i,y_j)\in \Gamma_3^{N,N}, \\ \mathcal{B}_4^{N,N} P_3(x_i,y_j)=-\mathcal{B}_4^{N,N} S_6(x_i,y_j), \ \mathcal{B}_4^{N,N} P_4(x_i,y_j)=-\mathcal{B}_4^{N,N} S_8(x_i,y_j), \quad \text{for all } (x_i,y_j)\in \Gamma_4^{N,N}, \\ P_1(d_1,y_j)+S_1(d_1,y_j)=P_3(d_1,y_j)+S_3(d_1,y_j), \ P_3(d_1,y_j)+S_5(d_1,y_j)=P_4(d_1,y_j)+S_7(d_1,y_j), \\ P_1(x_i,d_2)+S_2(x_i,d_2)=P_3(x_i,d_2)+S_6(x_i,d_2), \ P_2(x_i,d_2)+S_4(x_i,d_2)=P_4(x_i,d_2)+S_8(x_i,d_2), \end{cases} \tag{4.3}$$

such that the discrete solution Z of (3.4) can be define as the following decomposition:

$$Z(x_i,y_j)=\begin{cases} R_1(x_i,y_j)+S_1(x_i,y_j)+P_1(x_i,y_j)+S_2(x_i,y_j), \quad \text{for } (x_i,y_j)\in \mathcal{D}_1^{N,N}, \\ R_2(x_i,y_j)+S_3(x_i,y_j)+P_2(x_i,y_j)+S_4(x_i,y_j), \quad \text{for } (x_i,y_j)\in \mathcal{D}_2^{N,N}, \\ R_3(x_i,y_j)+S_5(x_i,y_j)+P_3(x_i,y_j)+S_6(x_i,y_j), \quad \text{for } (x_i,y_j)\in \mathcal{D}_3^{N,N}, \\ R_4(x_i,y_j)+S_7(x_i,y_j)+P_4(x_i,y_j)+S_8(x_i,y_j), \quad \text{for } (x_i,y_j)\in \mathcal{D}_4^{N,N}, \\ [R(d_1,y_j)]+[S(d_1,y_j)]+[P(d_1,y_j)]=0, \\ [R(x_i,d_2)]+[S(x_i,d_2)]+[P(x_i,d_2)]=0, \end{cases} \tag{4.4}$$

where $R=\sum_{k=1}^4 R_k,\ S=\sum_{l=1}^8 S_l,\ P=\sum_{m=1}^4 P_m$.

Lemma 4.1. *Let the continuous regular components $r_k(x,y)$ are the solutions of problem (2.6) and the discrete regular components R_k are the numerical solutions of the problem (4.1); then, it holds*

$$|r_k(x_i,y_j)-R_k(x_i,y_j)|\le CN^{-1}, \ \forall (x_i,y_j)\in \overline{\mathfrak{D}}_k^{N,N}, \ k=1,2,3,4. \tag{4.5}$$

Proof. Note that the inequalities

$$\begin{cases} |\mathcal{B}_1^{N,N}(r_k(0,y_j)-R_k(0,y_j))|\le CN^{-1}, \ |\mathcal{B}_2^{N,N}(r_k(x_i,0)-R_k(x_i,0))|\le CN^{-1}, \\ |\mathcal{B}_3^{N,N}(r_k(1,y_j)-R_k(1,y_j))|\le CN^{-1}, \ |\mathcal{B}_4^{N,N}(r_k(x_i,1)-R_k(x_i,1))|\le CN^{-1}, \end{cases} \tag{4.6}$$

follow immediately from (4.1) and Theorem 2.4.
The truncation error related to the regular components R_k, $k=1,2,3,4$ on the subdomains $\mathcal{D}_k^{N,N}$, $k=1,2,3,4$ satisfies

$$|L_\varepsilon^{N,N}(r_k(x_i,y_j)-R_k(x_i,y_j))|\le C\varepsilon\left(\bar{h}_i\left\|\frac{\partial^3 r}{\partial x^3}\right\|+\bar{k}_j\left\|\frac{\partial^3 r}{\partial y^3}\right\|\right)+C\left(h_i\left\|\frac{\partial^2 r}{\partial x^2}\right\|+k_j\left\|\frac{\partial^2 r}{\partial y^2}\right\|\right),$$

and therefore it holds

$$|L_\varepsilon^{N,N}(r_k(x_i,y_j)-R_k(x_i,y_j))|\le CN^{-1},$$

and from the discrete maximum principle the required result follows. $\square$

To establish ε-uniform bounds on the truncation errors for the components associated with the edges ad corner functions, we use the standard barrier functions given by

$$\begin{cases} \mathcal{G}_{s_1;i}=\prod_{v=i}^{N/2}\left(1+h_v\frac{\alpha}{2\varepsilon}\right)^{-1}, & \text{for } i=1,2,\dots,N/2,\ j=1,2,\dots,N/2, \\ \mathcal{G}_{s_2;j}=\prod_{v=j}^{N/2}\left(1+k_v\frac{\beta}{2\varepsilon}\right)^{-1}, & \text{for } i=1,2,\dots,N/2,\ j=1,2,\dots,N/2, \\ \mathcal{G}_{p_1;i,j}=\prod_{v=i}^{N/2}\left(1+h_v\frac{\alpha}{2\varepsilon}\right)^{-1}\prod_{v=j}^{N/2}\left(1+k_v\frac{\beta}{2\varepsilon}\right)^{-1}, & \text{for } i=1,2,\dots,N/2,\ j=1,2,\dots,N/2, \end{cases}$$

$$\begin{cases} \mathcal{G}_{s_3;i}=\prod_{v=i}^{N}\left(1+h_v\frac{\alpha}{2\varepsilon}\right)^{-1}, & \text{for } i=N/2+1,\dots,N,\ j=1,2,\dots,N/2, \\ \mathcal{G}_{s_4;j}=\prod_{v=j}^{N/2}\left(1+k_v\frac{\beta}{2\varepsilon}\right)^{-1}, & \text{for } i=N/2+1,\dots,N,\ j=1,2,\dots,N/2, \\ \mathcal{G}_{p_2;i,j}=\prod_{v=i}^{N}\left(1+h_v\frac{\alpha}{2\varepsilon}\right)^{-1}\prod_{v=j}^{N/2}\left(1+k_v\frac{\beta}{2\varepsilon}\right)^{-1}, & \text{for } i=N/2+1,\dots,N,\ j=1,2,\dots,N/2, \end{cases}$$

$$\begin{cases} \mathcal{G}_{s_5;i}=\prod_{v=i}^{N/2}\left(1+h_v\frac{\alpha}{2\varepsilon}\right)^{-1}, & \text{for } i=1,\dots,N/2,\ j=N/2+1,\dots,N, \\ \mathcal{G}_{s_6;j}=\prod_{v=j}^{N}\left(1+k_v\frac{\beta}{2\varepsilon}\right)^{-1}, & \text{for } i=1,\dots,N/2,\ j=N/2+1,\dots,N, \\ \mathcal{G}_{p_3;i,j}=\prod_{v=i}^{N/2}\left(1+h_v\frac{\alpha}{2\varepsilon}\right)^{-1}\prod_{v=j}^{N}\left(1+k_v\frac{\beta}{2\varepsilon}\right)^{-1}, & \text{for } i=1,\dots,N/2,\ j=N/2+1,\dots,N, \end{cases}$$

$$\begin{cases} \mathcal{G}_{s_7;i} = \prod_{v=i}^{N} \left(1 + h_v \frac{\alpha}{2\varepsilon}\right)^{-1}, & \text{for } i = N/2+1,\dots,N,\ j = N/2+1,\dots,N, \\ \mathcal{G}_{s_8;j} = \prod_{v=j}^{N} \left(1 + k_v \frac{\beta}{2\varepsilon}\right)^{-1}, & \text{for } i = N/2+1,\dots,N,\ j = N/2+1,\dots,N, \\ \mathcal{G}_{p_4;i,j} = \prod_{v=i}^{N} \left(1 + h_v \frac{\alpha}{2\varepsilon}\right)^{-1} \prod_{v=j}^{N} \left(1 + k_v \frac{\beta}{2\varepsilon}\right)^{-1}, & \text{for } i = N/2+1,\dots,N,\ j = N/2+1,\dots,N. \end{cases}$$

These functions are first order Taylor series of the exponential functions related to the singular component of the problem (1.1). For any grid point $(x_i, y_j) \in \mathcal{D}_1^{N,N}$, we have

$$|S_1(x_i, y_j)| \le \mathcal{G}_{s_1;i},\ |S_2(x_i, y_j)| \le \mathcal{G}_{s_2;j},\ |P_1(x_i, y_j)| \le \mathcal{G}_{p_1;i,j}. \tag{4.7}$$

For $i = 1,\dots,N/4$, $j = 1,\dots,N/2$, we get

$$\mathcal{G}_{s_1;i} \le \mathcal{G}_{s_1;N/4} \le C \exp\left(\sum_{v=N/4}^{N/2} \left(\frac{1}{2}\left(\frac{\alpha h_v}{2\varepsilon}\right)^2 - \frac{\alpha h_v}{2\varepsilon} \right) \right) \le C N^{-1}. \tag{4.8}$$

For $i = 1,\dots,N/2$, $j = 1,\dots,N/4$, we have

$$\mathcal{G}_{s_2;j} \le \mathcal{G}_{s_2;N/4} \le C \exp\left(\sum_{v=N/4}^{N/2} \left(\frac{1}{2}\left(\frac{\alpha k_v}{2\varepsilon}\right)^2 - \frac{\alpha k_v}{2\varepsilon} \right) \right) \le C N^{-1}. \tag{4.9}$$

For $i = 1,\dots,N/4$, $j = 1,\dots,N/4$, we have

$$\mathcal{G}_{p_1;i,j} \le \mathcal{G}_{p_1;N/4,N/4} \le C \exp\left(\sum_{v=N/4}^{N/2} \left(\frac{1}{2}\left(\frac{\alpha h_v}{2\varepsilon}\right)^2 - \frac{\alpha h_v}{2\varepsilon} \right) + \sum_{v=N/4}^{N/2} \left(\frac{1}{2}\left(\frac{\alpha k_v}{2\varepsilon}\right)^2 - \frac{\alpha k_v}{2\varepsilon} \right) \right) \le C N^{-1}. \tag{4.10}$$

Similarly, bounds exist for the remaining layer components.

Lemma 4.2. *Let s_l are the solutions of the problem (2.8) and S_l are the solutions of the problem (4.2), then, for $l = 1,\dots,8$, it holds*

$$|s_l(x_i, y_j) - S_l(x_i, y_j)| \le C N^{-1} \ln N, \textit{ for } (x_i, y_j) \in \mathcal{D}_k^{N,N},\ k = 1,2,3,4. \tag{4.11}$$

Proof. First, note the inequalities for the interior layer component s_1 on the boundaries of subdomain $\mathcal{D}_1^{N,N}$, such as

$$|\mathcal{B}_1^{N,N}(s_1(0, y_j) - S_1(0, y_j))| \le C N^{-1},\ |\mathcal{B}_2^{N,N}(s_1(x_i, 0) - S_1(x_i, 0))| \le C N^{-1}, \tag{4.12}$$

which follow from (4.2) and Theorem 2.4.

If $\tau_x = \frac{d_1}{2}$, standard procedures can be used to obtain the proof by noting that $\varepsilon^{-1} \le C \ln N$. Hereby, we will assume that $\tau_x = \frac{2\varepsilon}{\alpha} \ln N$. Here we merely give the details of the proof corresponding to the layer function s_1.

Using Theorem 2.4 and (4.7), we can deduce

$$|s_1(x_i, y_j) - S_1(x_i, y_j)| \le |s_1(x_i, y_j)| + |S_1(x_i, y_j)| \le C \exp(-\alpha \tau_x/\varepsilon) + \mathcal{G}_{s_1;i}.$$

From (4.8), it follows

$$|s_1(x_i, y_j) - S_1(x_i, y_j)| \le C N^{-1},\ i = 1,\dots,N/4,\ j = 1,\dots,N/2. \tag{4.13}$$

We proceed in the following manner to prove equivalent error bounds in the region $\mathcal{D}_{1,1}^{N,N} = \{(x_i, y_j) | \frac{N}{4} < i < \frac{N}{2},\ 0 < j < \frac{N}{2}\}$. Using Taylor series, we obtain

$$|L_\varepsilon^{N,N}(s_1(x_i, y_j) - S_1(x_i, y_j))| \le C N^{-1} \tau_x \left(\varepsilon \left\| \frac{\partial^3 s_1}{\partial x^3} \right\| + \left\| \frac{\partial^2 s_1}{\partial x^2} \right\| \right) + C N^{-1} \left(\varepsilon \left\| \frac{\partial^3 s_1}{\partial y^3} \right\| + \left\| \frac{\partial^2 s_1}{\partial y^2} \right\| \right).$$

With the help of derivative's bounds of s_1 given in Theorem 2.4, we obtain the following estimate

$$|L_\varepsilon^{N,N}(s_1(x_i, y_j) - S_1(x_i, y_j))| \le C N^{-1} \ln N.$$

Hence, using the discrete maximum principle Lemma 3.1, we get the error bound on the domain $\bar{\mathcal{D}}_{1,1}^{N,N}$ as

$$|s_1(x_i, y_j) - S_1(x_i, y_j)| \le C N^{-1} \ln N. \tag{4.14}$$

The result follows from (4.13) and (4.14).

Likewise, we can obtain similar bounds for the errors associate to the remaining layer components s_l, $l = 2,\dots,8$ on the subdomains $\mathcal{D}_k^{N,N}$, $k = 1,2,3,4$. $\square$

Lemma 4.3. *Let p_m are the solutions of problem (2.12) and P_m are the solutions of problem (4.3), then, for $m = 1,2,3,4$, it holds*

$$|p_m(x_i, y_j) - P_m(x_i, y_j)| \le C N^{-1} \ln N, \textit{ for } (x_i, y_j) \in \mathcal{D}_k^{N,N},\ k = 1,2,3,4. \tag{4.15}$$

Proof. First, note the inequalities for the corner layer component p_1 on the boundaries of subdomain $\mathcal{D}_1^{N,N}$, such as

$$|\mathcal{B}_1^{N,N}(p_1(0,y_j)-P_1(0,y_j))| \le CN^{-1},\ |\mathcal{B}_2^{N,N}(p_1(x_i,0)-P_1(x_i,0))| \le CN^{-1}, \tag{4.16}$$

which follow from (4.3) and Theorem 2.4.

Here, for the corner layer component p_1, we merely present the proof of (4.15). Using Theorem 2.4 and (4.7), we obtain

$$|p_1(x_i,y_j)-P_1(x_i,y_j)| \le |p(x_i,y_j)| + |P_1(x_i,y_j)| \le C\exp(-\alpha\tau_x/\varepsilon)\exp(-\beta\tau_y/\varepsilon) + \mathcal{G}_{p_1;i,j}.$$

From (4.10), we prove

$$|p_1(x_i,y_j)-P_1(x_i,y_j)| \le CN^{-1},\ i=1,\dots,N/4,\ j=1,\dots,N/4. \tag{4.17}$$

In the domain $\mathcal{D}_{1,2}^{N,N} = \{(x_i,y_j)| \frac{N}{4} < i < \frac{N}{2},\ \frac{N}{4} < j < \frac{N}{2}\}$, the truncation error holds

$$\begin{aligned}|L_\varepsilon^{N,N}(p_1(x_i,y_j)-P_1(x_i,y_j))| &\le CN^{-1}\tau_x\left(\varepsilon\left\|\frac{\partial^3 p_1}{\partial x^3}\right\| + \left\|\frac{\partial^2 p_1}{\partial x^2}\right\|\right) + CN^{-1}\tau_y\left(\varepsilon\left\|\frac{\partial^3 p_1}{\partial y^3}\right\| + \left\|\frac{\partial^2 p_1}{\partial y^2}\right\|\right),\\ &\le C\varepsilon N^{-1}\ln N.\end{aligned}$$

Using the suitable barrier function $\Phi^{\pm}(x_i,y_j) = C\left(\frac{\tau_x N^{-1}}{\varepsilon}(x_i-d_1) + \frac{\tau_y N^{-1}}{\varepsilon}(y_j-d_2)\right) \pm (p_1(x_i,y_j)-P_1(x_i,y_j))$ and apply the Lemma 3.1, used on $\bar{\mathcal{D}}_{1,2}^{N,N}$, we get

$$|p_1(x_i,y_j)-P_1(x_i,y_j)| \le CN^{-1}\ln N. \tag{4.18}$$

The result follows from (4.17) and (4.18).

Likewise, we can obtain similar bounds for the errors associate to the remaining corner layer components p_m, $m=2,3,4$ on the subdomains $\mathcal{D}_k^{N,N}$, $k=2,3,4$. □

Theorem 4.4. *Let z be the exact solution of the continuous problem (1.1) and Z the numerical solution of the finite difference scheme (3.4) constructed on the Shishkin mesh given by the tensorial product of meshes defined in (3.3); then, it holds*

$$|z(x_i,y_j)-Z(x_i,y_j)| \le CN^{-1}\ln^2 N,\ \forall (x_i,y_j)\in \bar{\mathfrak{D}}^{N,N}, \tag{4.19}$$

where C is a positive constant independent of ε and N. Therefore, the numerical algorithm is an almost first order uniformly convergent method.

Proof. From Lemmas 4.1, 4.2 and 4.3, we deduce the following result of convergence

$$|z(x_i,y_j)-Z(x_i,y_j)| \le CN^{-1}\ln N,\ \forall (x_i,y_j)\in \mathfrak{D}^{N,N}\setminus\{(d_1,y_j)\cup(x_i,d_2)\}, \tag{4.20a}$$

and from (4.6), (4.12), (4.16) and Lemma 2.3, we deduce the following result of convergence on the boundaries of the domain $\mathfrak{D}^{N,N}$ such as

$$|\mathcal{B}_1^{N,N}(z(0,y_j)-Z(0,y_j))| \le CN^{-1}\ln N,\ |\mathcal{B}_2^{N,N}(z(x_i,0)-Z(x_i,0))| \le CN^{-1}\ln N, \tag{4.20b}$$

$$|\mathcal{B}_3^{N,N}(z(1,y_j)-Z(1,y_j))| \le CN^{-1}\ln N,\ |\mathcal{B}_4^{N,N}(z(x_i,1)-Z(x_i,1))| \le CN^{-1}\ln N. \tag{4.20c}$$

On the other hand, at line $(x_i,y_j)=(d_1,y_j)$, it holds

$$\begin{aligned}|(D_x^+ - D_x^-)(z(d_1,y_j)-Z(d_1,y_j))| \le& |D_x^+ z(d_1,y_j) - \frac{\partial z}{\partial x}(d_1,y_j)| + |D_x^- z(d_1,y_j) - \frac{\partial z}{\partial x}(d_1,y_j)|\\ \le& (h_l+H_r)\frac{\partial^2 z}{\partial x^2}(d_1,y_j)\\ \le& (h_l+H_r)\varepsilon^{-2} \le C\frac{N^{-1}\ln N}{\varepsilon}.\end{aligned} \tag{4.21}$$

Using the suitable barrier function

$$\Phi(x_i,y_j) = C\frac{\tau_x N^{-1}}{\varepsilon^2}(x_i-(d_1-\tau_x)),\ (x_i,y_j)\in \mathcal{D}^{N,N}\cap(d_1-\tau_x,d_1)\times(0,1),$$

applying the Lemma 3.1 to $\Phi(x_i,y_j) \pm (z(d_1,y_j)-Z(d_1,y_j))$ over the interval $\bar{\mathcal{D}}^{N,N}\cap[d_1-\tau_x,d_1]\times[0,1]$, we obtain

$$|(z(d_1,y_j)-Z(d_1,y_j))| \le CN^{-1}\ln^2 N. \tag{4.22}$$

Similarly, we can prove for the discontinuous line $(x_i,y_j)=(x_i,d_2)$. Hence from (4.20) and (4.22), we can get the required result. □

5. Numerical experiments

In this Section, the proposed method is applied to two test problems. To see in practice that the numerical results are according with the theoretical results, we show tabular results for the errors and the orders of convergence. For simplicity, we take the same number of grid points at each spatial direction.

As the exact solutions are unknown for these problems, we use the double mesh principle (see [26]) to approximate the errors in the maximum norm. Then, the errors are approximated by

$$E_\varepsilon^{N,N} = \max_{(x_i,y_j)\in\bar{\mathfrak{D}}^{N,N}} |Z^{2N,2N}(x_{2i},y_{2j}) - Z^{N,N}(x_i,y_j)|$$

where $Z^{2N,2N}(x_{2i},y_{2j})$ represents the numerical solution to the problem (1.1) on a mesh with $2N$ partitions on each direction, which has the mesh points of the coarse mesh and their midpoints at each direction. The numerical orders of convergence are given by

$$Q_\varepsilon^{N,N} = \log_2\left(\frac{E_\varepsilon^{N,N}}{E_\varepsilon^{2N,2N}}\right).$$

The parameter maximum point-wise norm are determined by

$$E^{N,N} = \max_\varepsilon E_\varepsilon^{N,N}.$$

We also compute the uniform numerical orders of convergence in a standard way; they are given by

$$Q^{N,N} = \log_2\left(\frac{E^{N,N}}{E^{2N,2N}}\right).$$

Example 5.1. The first example is given by

$$-\varepsilon\left(\frac{\partial^2}{\partial x^2}+\frac{\partial^2}{\partial y^2}\right)z(x,y)+(1+x)\frac{\partial z(x,y)}{\partial x}+(1+y)\frac{\partial z(x,y)}{\partial y}+z(x,y)=f(x,y),\ \forall (x,y)\in\mathfrak{D},$$

where $d_1=0.5$, $d_2=0.5$, the source term is given by

$$f(x,y)=\begin{cases} f_1(x,y)=4\sin(\pi x)\sin(\pi y), & x\le d_1,\ y\le d_2,\\ f_2(x,y)=-3\sin(\pi(1-x))\sin(\pi y), & x>d_1,\ y\le d_2,\\ f_3(x,y)=8\sin(\pi x)\sin(\pi(1-y)), & x\le d_1,\ y>d_2,\\ f_4(x,y)=2\sin(\pi(1-x)\sin(\pi(1-y))), & x>d_1,\ y>d_2,\end{cases}$$

and the boundary conditions are

$$\begin{aligned} z(0,y)-\varepsilon\frac{\partial z(0,y)}{\partial x}&=0,\ z(1,y)+\varepsilon\frac{\partial z(1,y)}{\partial x}=(1-y),\\ z(x,0)-\varepsilon\frac{\partial z(x,0)}{\partial y}&=0,\ z(x,1)+\varepsilon\frac{\partial z(x,1)}{\partial y}=(1-x).\end{aligned}$$

Example 5.2. The second example is given by

$$-\varepsilon\left(\frac{\partial^2}{\partial x^2}+\frac{\partial^2}{\partial y^2}\right)z(x,y)+(1+x\sin(\pi y/4))\frac{\partial z(x,y)}{\partial x}+(1+y\exp(x))\frac{\partial z(x,y)}{\partial y}+(\exp(2y))z(x,y)=f(x,y),\ \forall (x,y)\in\mathfrak{D},$$

where now $d_1=0.4$, $d_2=0.6$, the source term is given by

$$f(x,y)=\begin{cases} f_1(x,y)=xy\sin(\pi x)\cos(\pi y/2), & x\le d_1,\ y\le d_2,\\ f_2(x,y)=(1-x)y\sin(\pi(x-d_1))\cos(\pi y/2), & x>d_1,\ y\le d_2,\\ f_3(x,y)=x(1-y)\sin(\pi x)\cos(\pi(y-d_2)/2), & x\le d_1,\ y>d_2,\\ f_4(x,y)=(1-x)(1-y)\sin(\pi(x-d_1))\cos(\pi(y-d_1)/2), & x>d_1,\ y>d_2,\end{cases}$$

and the boundary conditions are

$$\begin{aligned} z(0,y)-\varepsilon\frac{\partial z(0,y)}{\partial x}&=0,\ z(1,y)+\varepsilon\frac{\partial z(1,y)}{\partial x}=0,\\ z(x,0)-\varepsilon\frac{\partial z(x,0)}{\partial y}&=0,\ z(x,1)+\varepsilon\frac{\partial z(x,1)}{\partial y}=0.\end{aligned}$$

In Tables 1 and 2 we have chosen $\varepsilon=2^{-3k}$, $k=0,\ldots,8$, using the finite-difference method (FDM) on the Shishkin mesh. These tables show the maximum point-wise errors and the orders of convergence corresponding to Example 5.1 and Example 5.2 respectively. Further, from Tables 1 and 2, it is clear that our numerical scheme is an almost first-order uniformly convergent method. Figs. 2a and 3a display the numerical solution of Problems 5.1 and 5.2 respectively, for $\varepsilon=2^{-6}$ and $N=128$; from them, we clearly see the boundary and the interior layers in both cases. Due to the appearance of these layers, the errors are significantly large in these regions, as we can observe in Figs. 4a and 5a for Examples 5.1 and 5.2, respectively.

Remark 5.1. In the future, we intend to analyze the uniform convergence on other special meshes, such as Bakhvalov, Gartland, or Duran-Shishkin meshes. Here, we have included the numerical solution and computed error solution graphs, for both examples, to substantiate the difference between the Bakhvalov-Shishkin and Shishkin meshes (see the Figs. 2, 3, 4 and 5). In addition, we have observed that the variation of the present scheme can also capture the boundary and interior layers based on the several possible changes of sign at the point of discontinuities on the convection coefficients. It is to be noted that the current problem can be also extended to elliptic interface problems with complicated domain, having interface on a curve based, by using some suitable transformations. The current problem relies on a linear setup with Robin-type boundary conditions that may be generalized to nonlinear situations by linearization techniques under suitable conditions. This will also be considered in our future works.

Table 1
Orders of convergence $Q^{N,N}$ and maximum point-wise errors $E^{N,N}$ for Example 5.1.

ε/ N	32	64	128	256	512	1024
2^0	3.003e-2	1.652e-2	8.640e-3	4.416e-3	2.232e-3	1.122e-3
$Q_\varepsilon^{N,N}$	0.86219	0.9347	0.9682	0.9844	0.9922	-
2^{-3}	5.534e-2	3.016e-2	1.589e-2	8.190e-3	4.162e-3	2.098e-3
$Q_\varepsilon^{N,N}$	0.87569	0.9246	0.9564	0.9767	0.9879	-
2^{-6}	1.264e-1	8.662e-2	5.630e-2	3.519e-2	2.091e-2	1.198e-2
$Q_\varepsilon^{N,N}$	0.54522	0.6217	0.6778	0.7514	0.8035	-
2^{-9}	1.448e-1	1.006e-1	6.439e-2	3.998e-2	2.347e-2	1.333e-2
$Q_\varepsilon^{N,N}$	0.52543	0.6436	0.6876	0.7684	0.8160	-
2^{-12}	1.479e-1	1.032e-1	6.593e-2	4.097e-2	2.402e-2	1.364e-2
$Q_\varepsilon^{N,N}$	0.51918	0.6459	0.6863	0.7703	0.8160	-
2^{-15}	1.483e-1	1.035e-1	6.616e-2	4.110e-2	2.410e-2	1.369e-2
$Q_\varepsilon^{N,N}$	0.51889	0.6457	0.6867	0.7705	0.8160	-
2^{-18}	1.483e-1	1.035e-1	6.619e-2	4.112e-2	2.411e-2	1.369e-2
$Q_\varepsilon^{N,N}$	0.51889	0.6457	0.6867	0.7705	0.8160	-
2^{-21}	1.484e-1	1.036e-1	6.619e-2	4.112e-2	2.411e-2	1.369e-2
$Q_\varepsilon^{N,N}$	0.51847	0.6456	0.6867	0.7705	0.8160	-
2^{-24}	1.484e-1	1.036e-1	6.619e-2	4.112e-2	2.411e-2	1.369e-2
$Q_\varepsilon^{N,N}$	0.51847	0.6456	0.6867	0.7705	0.8160	-
$E^{N,N}$	1.484e-1	1.036e-1	6.619e-2	4.112e-2	2.411e-2	1.369e-2
$Q^{N,N}$	0.51847	0.6456	0.6867	0.7705	0.8160	-

Table 2
Orders of convergence $Q^{N,N}$ and maximum point-wise errors $E^{N,N}$ for Example 5.2.

ε/ N	32	64	128	256	512	1024
2^0	3.669e-4	1.891e-4	9.913e-5	5.074e-5	2.567e-5	1.291e-5
$Q_\varepsilon^{N,N}$	0.95624	0.9316	0.9661	0.9831	0.9916	-
2^{-3}	6.148e-4	3.608e-4	1.998e-4	1.060e-4	5.474e-5	2.784e-5
$Q_\varepsilon^{N,N}$	0.76892	0.8524	0.9146	0.9535	0.9755	-
2^{-6}	1.344e-3	9.902e-4	6.789e-4	4.568e-4	2.879e-4	1.692e-4
$Q_\varepsilon^{N,N}$	0.44074	0.5445	0.5716	0.6662	0.7670	-
2^{-9}	1.446e-3	1.071e-3	7.294e-4	4.820e-4	2.990e-4	1.764e-4
$Q_\varepsilon^{N,N}$	0.43311	0.5545	0.5977	0.6891	0.7611	-
2^{-12}	1.459e-3	1.084e-3	7.378e-4	4.847e-4	2.983e-4	1.748e-4
$Q_\varepsilon^{N,N}$	0.42862	0.5547	0.6062	0.7002	0.7711	-
2^{-15}	1.460e-3	1.085e-3	7.389e-4	4.849e-4	2.980e-4	1.743e-4
$Q_\varepsilon^{N,N}$	0.42827	0.5547	0.6076	0.7025	0.7734	-
2^{-18}	1.461e-3	1.086e-3	7.390e-4	4.850e-4	2.979e-4	1.743e-4
$Q_\varepsilon^{N,N}$	0.42793	0.5547	0.6078	0.7028	0.7738	-
2^{-21}	1.461e-3	1.086e-3	7.390e-4	4.850e-4	2.979e-4	1.743e-4
$Q_\varepsilon^{N,N}$	0.42793	0.5547	0.6078	0.7029	0.7738	-
2^{-24}	1.461e-3	1.086e-3	7.390e-4	4.850e-4	2.979e-4	1.743e-4
$Q_\varepsilon^{N,N}$	0.42793	0.5547	0.6078	0.7029	0.7738	-
$E^{N,N}$	1.461e-3	1.086e-3	7.390e-4	4.850e-4	2.979e-4	1.743e-4
$Q^{N,N}$	0.42793	0.5547	0.6078	0.7029	0.7738	-

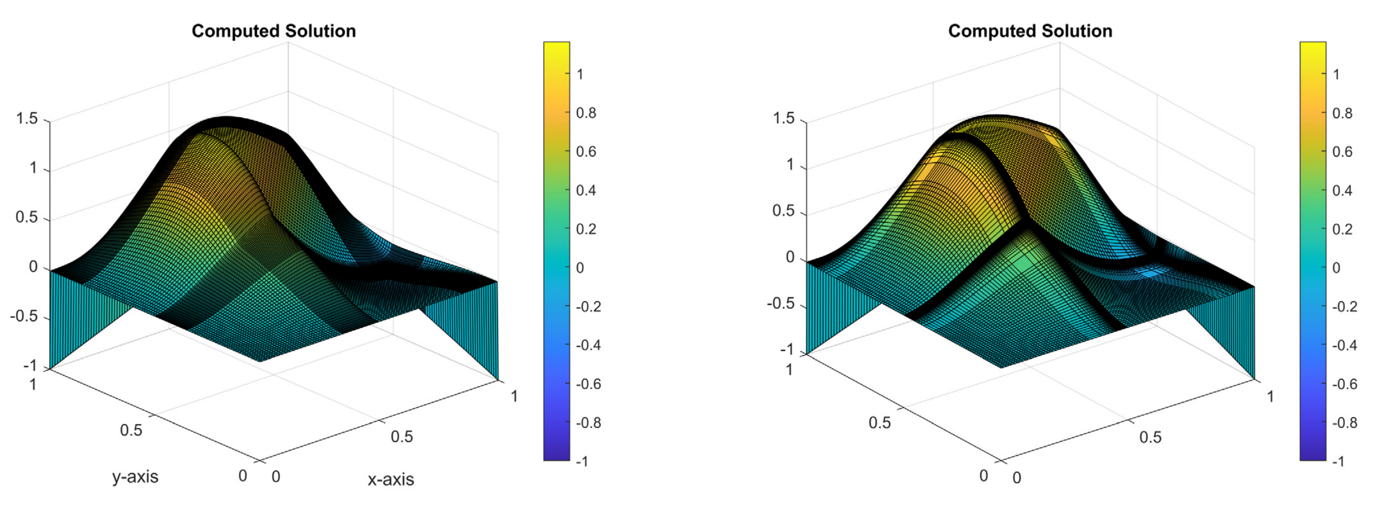

(a) Surface graph of the numerical solution Z using the S-mesh (b) Surface graph of the numerical solution Z using the B-S-mesh

Fig. 2. Surface graph with weak-interior layers of the numerical solution Z for Example 5.1, when $\varepsilon = 2^{-6}$, $N = 128$, $d_1 = 0.5, d_2 = 0.5$.

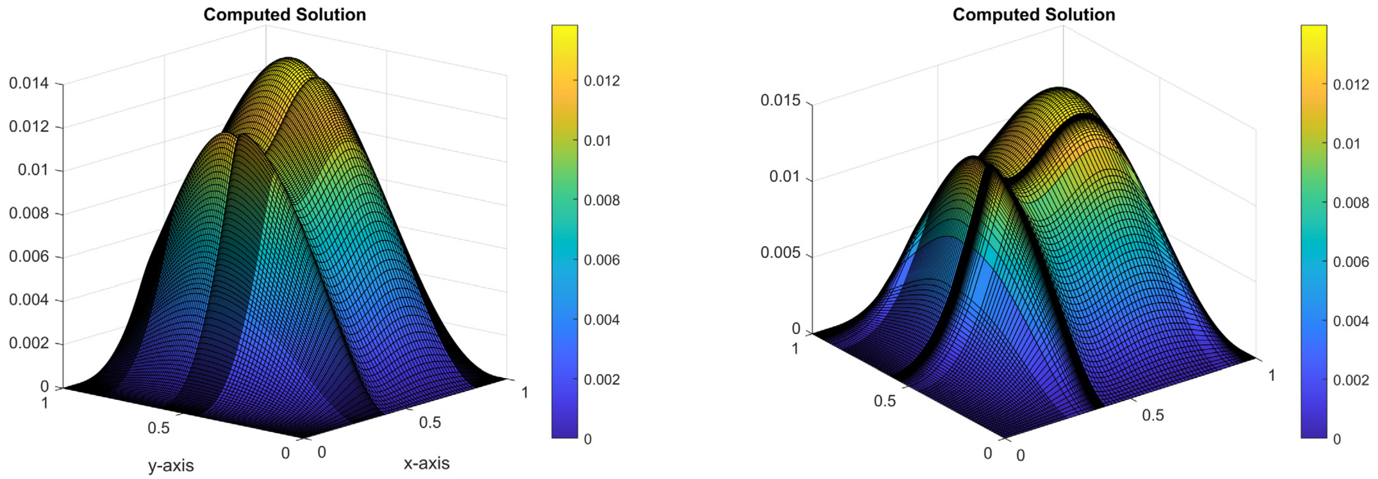

(a) Surface graph of the numerical solution Z using the S-mesh

(b) Surface graph of the numerical solution Z using the B-S-mesh

Fig. 3. Surface graph with weak-interior layers of the numerical solution Z for Example 5.2, when $\varepsilon = 2^{-6}, N = 128,\ d_1 = 0.4, d_2 = 0.6$.

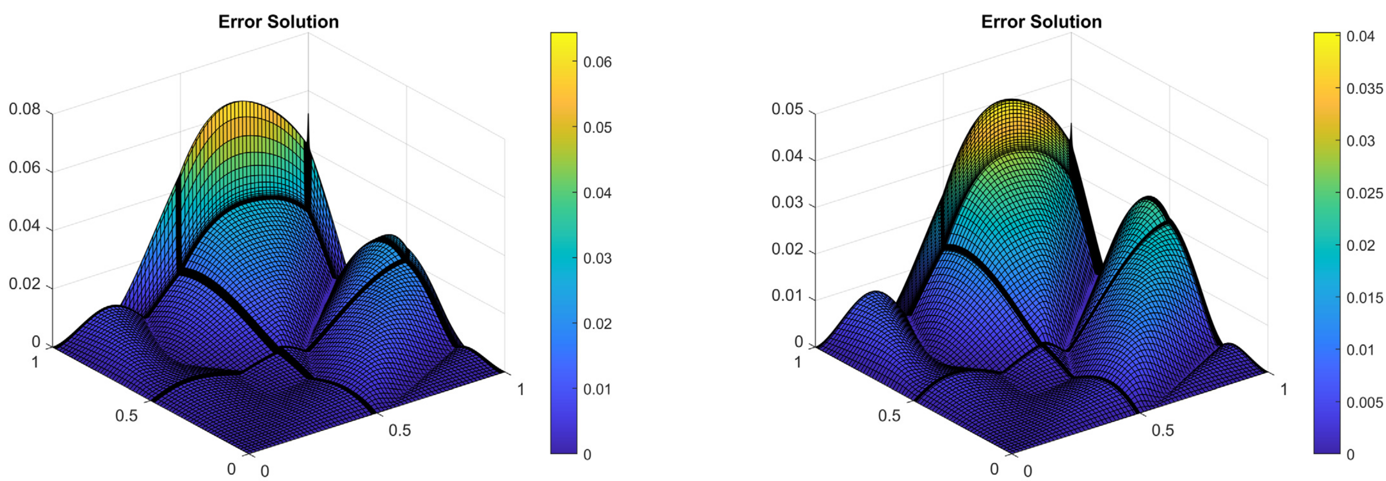

(a) Error graph of the numerical solution using the S-mesh

(b) Error graph of the numerical solution using the B-S-mesh

Fig. 4. Error of the numerical solution Z of the numerical solution Z for Example 5.1, when $\varepsilon = 2^{-6}, N = 128,\ d_1 = 0.5, d_2 = 0.5$.

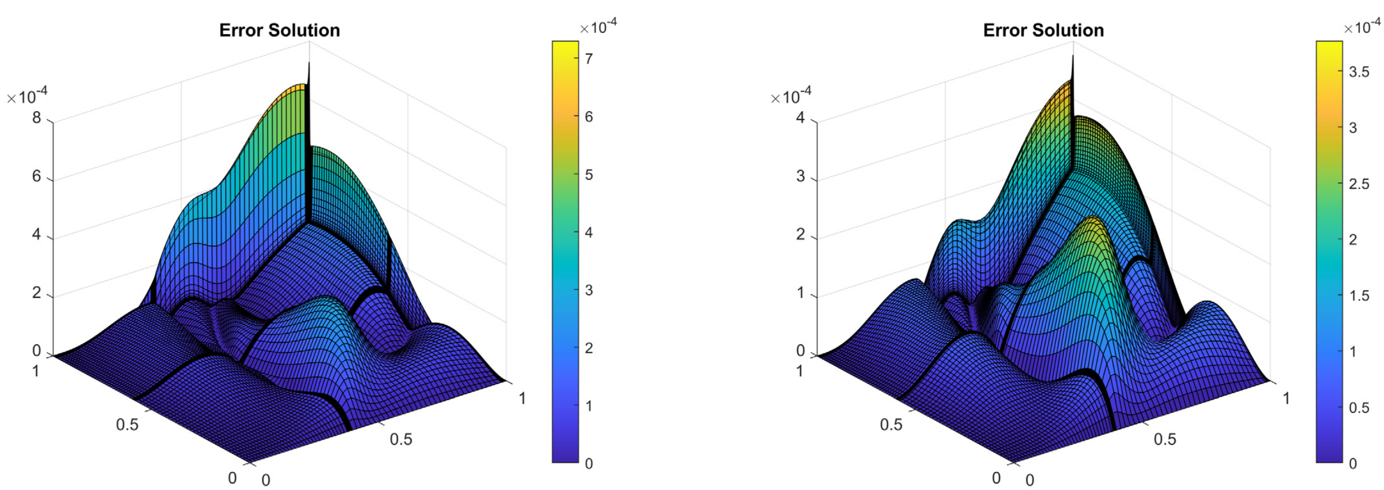

(a) Error graph of the numerical solution using the S-mesh

(b) Error graph of the numerical solution using the B-S-mesh

Fig. 5. Error of the numerical solution Z for Example 5.2, when $\varepsilon = 2^{-6}, N = 128,\ d_1 = 0.4, d_2 = 0.6$.

Data availability

No data was used for the research described in the article.

Acknowledgements

This research was partially supported by the project MTM2017-83490-P, the Aragón Government and European Social Fund (group E24-17R) and the Public University of Navarra (PRO-UPNA (6158)). This research is also supported by the Ministry of Education, Government of India for the second author.

References

[1] R.E. O'Malley Jr, Introduction to Singular Perturbations, Tech. Rep., 1974.
[2] H. Schlichting, K. Gersten, Boundary-Layer Theory, MacGraw Hill, New York, 1979.
[3] S. Srivastava, A. Verma, M. Kumar, An elliptic interface problem: a review, Appl. Math. Inf. Sci. Lett. 7 (3) (2019) 51–59.
[4] A. Taigbenu, J.A. Liggett, An integral solution for the diffusion-advection equation, Water Resour. Res. 22 (8) (1986) 1237–1246.
[5] H.G. Roos, M. Stynes, L. Tobiska, Robust Numerical Methods for Singularly Perturbed Differential Equations, 2nd edition, Springer Series in Computational Mathematics, vol. 24, Springer-Verlag, Berlin, 2008.
[6] M. Stynes, D. Stynes, Convection-Diffusion Problems, Graduate Studies in Mathematics, vol. 196, American Mathematical Society/Atlantic Association for Research in the Mathematical Sciences (AARMS), Providence, RI/Halifax, NS, 2018.
[7] A.F. Hegarty, E. O'Riordan, M. Stynes, A comparison of uniformly convergent difference schemes for two-dimensional convection-diffusion problems, J. Comput. Phys. 105 (1) (1993) 24–32.
[8] C. Clavero, J. Gracia, E. O'Riordan, The defect-correction technique applied to singularly perturbed elliptic problems of convection-diffusion type, Monografías del Seminario Matemático García de Galdeano 33 (2006) 411–418.
[9] T. Linß, M. Stynes, Asymptotic analysis and Shishkin-type decomposition for an elliptic convection-diffusion problem, J. Math. Anal. Appl. 261 (2) (2001) 604–632.
[10] T.A. Nhan, R. Vulanović, The Bakhvalov mesh: a complete finite-difference analysis of two-dimensional singularly perturbed convection-diffusion problems, Numer. Algorithms 87 (1) (2021) 203–221.
[11] K.W. Morton, Revival: Numerical Solution of Convection-Diffusion Problems, CRC Press, 1996, 2019.
[12] S.C.S. Rao, A.K. Chaturvedi, Parameter-uniform numerical method for a two-dimensional singularly perturbed convection–reaction–diffusion problem with interior and boundary layers, Math. Comput. Simul. 187 (2021) 656–686.
[13] K. Aarthika, R. Shiromani, V. Shanthi, A higher-order finite difference method for two-dimensional singularly perturbed reaction-diffusion with source-term-discontinuous problem, Comput. Math. Appl. 118 (2022) 56–73.
[14] P.W. Hemker, G.I. Shishkin, L.P. Shishkina, High-order time-accurate schemes for singularly perturbed parabolic convection-diffusion problems with Robin boundary conditions, Comput. Methods Appl. Math. 2 (1) (2002) 3–25.
[15] S. Kumar, Sumit, H. Ramos, Parameter-uniform approximation on equidistributed meshes for singularly perturbed parabolic reaction-diffusion problems with Robin boundary conditions, Appl. Math. Comput. 392 (2021) 125677.
[16] A.R. Ansari, A.F. Hegarty, Numerical solution of a convection diffusion problem with Robin boundary conditions, J. Comput. Appl. Math. 156 (1) (2003) 221–238.
[17] N.A. Mbroh, S.C.O. Noutchie, R.Y.M. Massoukou, A uniformly convergent finite difference scheme for Robin type singularly perturbed parabolic convection diffusion problem, Math. Comput. Simul. 174 (2020) 218–232.
[18] S. Natesan, N. Ramanujam, Initial-value technique for singularly perturbed boundary-value problems for second-order ordinary differential equations arising in chemical reactor theory, J. Optim. Theory Appl. 97 (2) (1998) 455–470.
[19] H. Han, R.B. Kellogg, Differentiability properties of solutions of the equation $-\epsilon^2\Delta u + ru = f(x,y)$ in a square, SIAM J. Math. Anal. 21 (2) (1990) 394–408.
[20] F. Liu, N. Madden, M. Stynes, A. Zhou, A two-scale sparse grid method for a singularly perturbed reaction–diffusion problem in two dimensions, IMA J. Numer. Anal. 29 (4) (2009) 986–1007.
[21] P. Farrell, A. Hegarty, J. Miller, E. O'Riordan, G. Shishkin, Singularly perturbed parabolic convection-diffusion problems with boundary and weak interior layers, J. Comput. Appl. Math. 166 (2004) 133–151.
[22] J.J.H. Miller, E. O'Riordan, G.I. Shishkin, Fitted Numerical Methods for Singular Perturbation Problems: Error Estimates in the Maximum Norm for Linear Problems in One and Two Dimensions, World Scientific, 1996.
[23] G. Shishkin, L. Shishkina, Difference Methods for Singular Perturbation Problems, Monographs and Surveys in Pure and Applied Mathematics, vol. 140, Chapamn & Hall/CRC, 2009.
[24] O. Ladyzhenskaya, V. Solonikov, N. Uraltseva, Linear and Quasilinear Equations of Parabolic Type, Translations of Mathematical Monographs, vol. 23, American Mathematical Society, 1967.
[25] O.A. Ladyzhenskaya, N.N. Ural'tseva, Linear and Quasilinear Elliptic Equations, Academic Press, New York, 1968.
[26] P. Farrell, A. Hegarty, J.J.H. Miller, E. O'Riordan, G.I. Shishkin, Robust Computational Techniques for Boundary Layers, CRC Press, 2000.